KIND, R. and G. MÜLLER (1975): Computations of SV waves in realistic Earth models, *J. Geophys.*, **41**, 149-172.
LAY, T. and D.V. HELMBERGER (1983): The shear wave velocity gradient at the base of the mantle, *J. Geophys. Res.*, **88**, 8160-8170.
MASTERS, T.G., H. BOLTON and P.M. SHEARER (1992): Large-scale 3 dimensional structure of the mantle (abstract), *EOS, Trans.* AGU., **73**, 201.
MITCHELL, B.J. and D.V. HELMBERGER (1973): Shear velocities at the base of the mantle from observations of S and ScS, *J. Geophys. Res.*, **78**, 6009-6020.
RICHARDS, P.G., D.C. WITTE and G. EKSTROM (1991): Generalized ray theory for seismic waves in structures with planar nonparalleled interfaces, *Bull. Seism. Soc. Am.*, **81**, 1309-1331.
SILVER, P. and C.R. BINA (1993): An anomaly in the amplitude ratio of SKKS/SKS in the range 100-108° from portable teleseismic data, *Geophys. Res. Lett.* (in press).
SIPKIN, S.A. and T.H. JORDAN (1980): Multiple ScS travel times in the Western Pacific: Implications for mantle heterogeneity, *J. Geophys. Res.*, **85**, 853-861.
STEAD, R.J. and D.V. HELMBERGER (1988): Numerical-analytical interfacing in two-dimensions with applications to modeling NTS seismograms, *PAGEOPH*, **128**, 157-193.
SU, W.J. and A.M. DZIEWONSKI (1994): Degree 12 model of shear velocity heterogeneity in the mantle, *J. Geophys. Res.*, **99**, 6945-6980.
TANIMOTO, T. (1990): Long-wavelength *S*-wave velocity structure throughout the mantle, *Geophys. J. Int.*, **100**, 327-336.
VIDALE, J., D.V. HELMBERGER and R.W. CLAYTON (1985): Finite-difference seismograms for SH-waves. *Bull. Seism. Soc. Am.*, **75**, 1765-1782.
WEBER, M. and J.P. DAVIS (1990): Evidence of a laterally variable lower mantle structure from *P*- and *S*-waves, *Geophys. J. Int.*, **102**, 231-255.
WIGGINS, R.A. (1976): Body wave amplitude calculations, II, *Geophys. J. R. Astron. Soc.*, **46**, 1-10.
WIGGINS, R.A. and J.A. MADRID (1974): Body wave amplitude calculations, *Geophys. J. R. Astron. Soc.*, **37**, 423-433.
YOUNG, C.J. and T. LAY (1987): Evidence for a shear velocity discontinuity in the lower mantle beneath India and the Indian Ocean, *Phys. Earth Planet. Inter.*, **49**, 37-53.
ZHANG, J. and T. LAY (1984): Investigation of a lower mantle shear wave triplication using broadband array, *Geophys. Res. Lett.*, **11**, 620-623.

SEISMIC MODELLING OF EARTH STRUCTURE
Eds. Enzo Boschi, Göran Ekström and Andrea Morelli

6
Seismic ray tracing

JEAN VIRIEUX
Institut Universitaire de France, Université de Nice - Sophia Antipolis, 06560 Valbonne, France

6.1 Introduction

Our object of investigation is the Earth at different scales: global, regional and local scales. We are interested in the propagation of seismic signals in the complex media which is the Earth. Records have been obtained for the Moon, while projects are under investigation for Mars and Venus. In the future, we might increase our interest for "planetary quakes" and see differences and common aspects of these different celestial bodies. Although these notes will essentially concentrate on methodological and technical aspects of the propagation, applications of the ray tracing theory at different scales will be mentioned in conclusion. Other lectures of this school have also illustrated many applications of high frequency theory in our understanding of earthquakes and structures.

The Earth is a mechanical body whose behaviour is complex and depends, in first approximation, on the time scale that one looks at the Earth and on the characteristic length related to this time scale by an appropriate velocity. For a characteristic time of a billion of years, the Earth behaves nearly as a drop of water. We progressively go through a visco-elastic behaviour for a time of millions of years for the crust and for a time of ten thousands of years for the mantle. For shorter periods between a few days and fractions of seconds, which correspond to the seismic window, the Earth behaves as an elastic body with a noticeable attenuation which must be taken into account. Except from the source area, where complex rheologies might take place in a few seconds, the response of the Earth is linear, which reduces the complexity of the different approaches we might consider. Let us emphasize that the seismic window is a very large window with more than 7 orders of magnitude in time. There are few domains in physics where such a widespread spectrum is valid for investigating a single object.

Our knowledge of the Earth interior since the beginning of the century has increased greatly. From a rather imprecise and poetic picture (Figure 6.1), the vertical structure has been refined from a global understanding (Figure 6.2) mainly

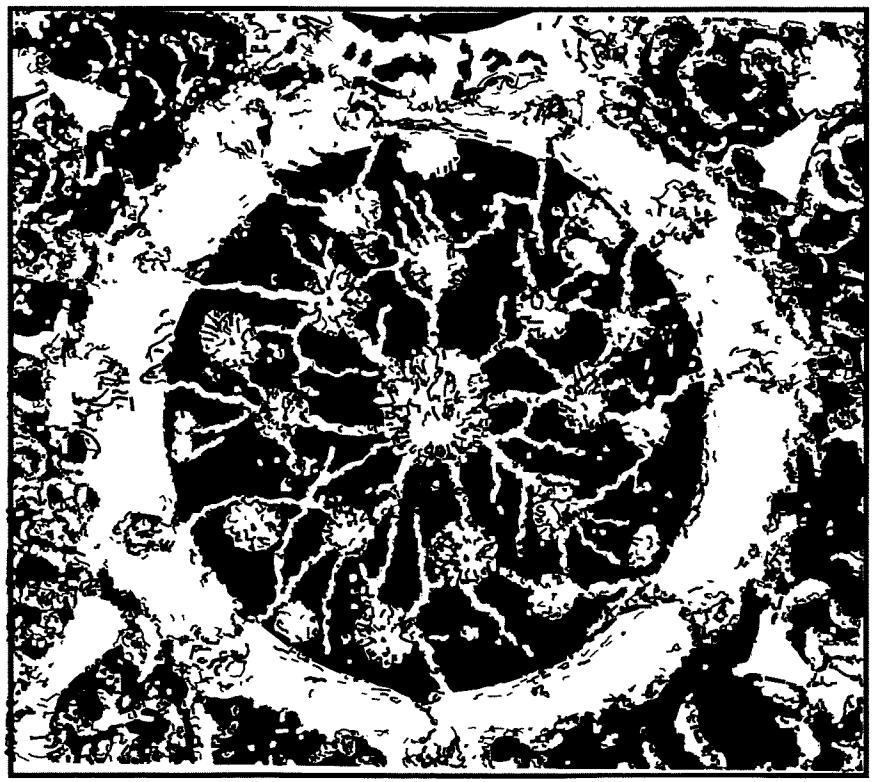

Figure 6.1 An early view (about 1800) of the Earth's interior considered as a ball of solid material fissured by tubes of magma, connecting pockets of eruptive gases to volcanic vents on the Earth's surface after *Inside the Earth* by Bolt (1982).

coming from astronomical studies to a more quantified picture (Figure 6.3) using essentially travel-time seismic data during the first half of this century. Only recent accumulation of data (see Dziewonski, 1996, for a review) as well as deeper analysis of these data has allowed an investigation of lateral variations (Figure 6.4).

Seismological data were crucial for this quantification: seismology is a very powerful tool for our knowledge of the Earth interior, because seismic waves go from one side to the other bringing to the surface the information they felt during their propagation. Other quantities as magnetic, electric or gravimetric fields allow different reconstruction of the Earth but none has the resolution of seismic waves, which is the reason of the importance of the seismic tool in the oil search in spite of a significant increase in cost. Electromagnetic waves are mainly diffused and not transported, while the gravimetric field suffers from the duality between the

distance and the importance of the anomalous density structure. This resolution power has a counter-part with the difficulty for the seismologist to interpret rather complex and deformed signals. This is why seismology, from my point of view, is so interesting.

In seismograms (as one calls time records for the global and regional scale) or traces (as one calls records for the local scale), two characteristic times appear: the time associated with the source signal which has a content of few seconds down to milliseconds and the time associated with the propagation which goes from hundred of seconds down to few seconds (Figures 6.5 and 6.6). For an opposite view, let us mention that recordings of the sea level do not exhibit this decoupling and are far more complex to analyze than seismograms. One must exploit deeply this advantage seen on seismograms: this is the reason why we should look carefully to the ray theory which is based explicitly on this decoupling between two time scales.

Neither the relative simplicity of the ray theory nor its computer efficiency make ray theory an often used technic in seismology, but its capacity for seismic interpretation. Let us underline that global models of Gutenberg and Jeffreys elaborated around 1940 (Bolt, 1982) are based on travel-time computed by ray

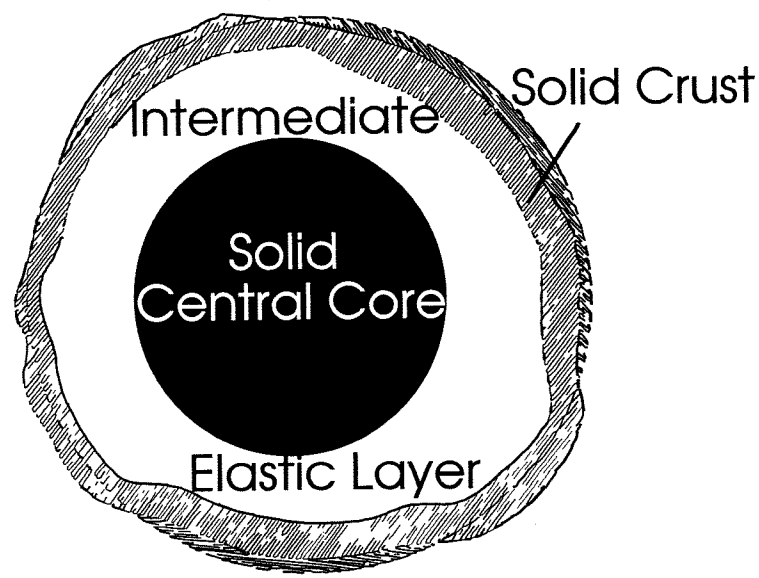

Figure 6.2 Sketch of the Earth's interior published in Berlin in 1902 by H. Kraemer. The Earth has three shells: a solid crust supported by an elastic intermediate layer wrapped around a solid central core. The change from the 18th century figure reflects an improved physical understanding essentially from astronomical data. The model is still limited by lack of seismological data after *Inside the Earth* by Bolt (1982).

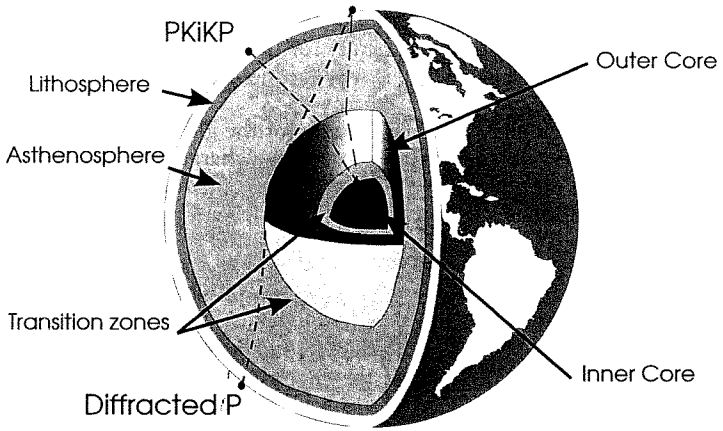

Figure 6.3 A cross section of the Earth based on the most recent seismological evidence. The outer shell consists of a rocky mantle that has structural discontinuities in its upper part and at its lower boundary that are capable of reflecting or modifying earthquake's waves. Below the mantle an outer fluid core surrounds a solid kernel at the Earth's center detected by reflected waves from the inner solid core labeled *PKiKP*; and the waves that creep around the liquid core are diffracted *P*. After *Inside the Earth* by Bolt (1982).

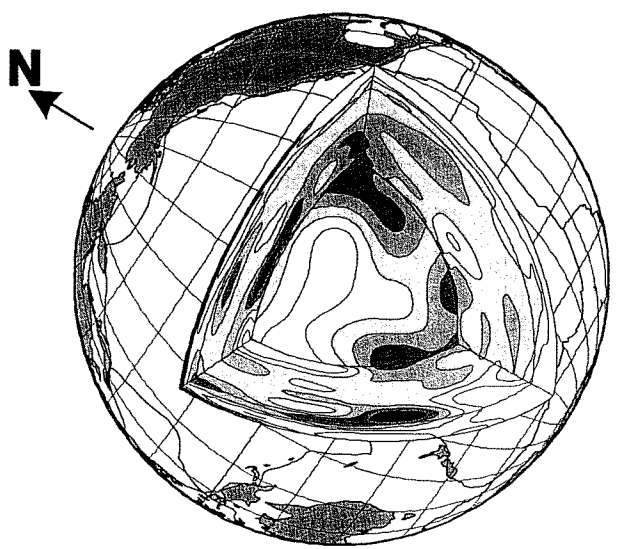

Figure 6.4 A cross section of the Earth showing a composite image synthesized from seismic tomographic mapping down to the core. Lateral variations are displayed with a gray scale and show the complexity of the *S* wave velocity inside the Earth after Su *et al.* (1994).

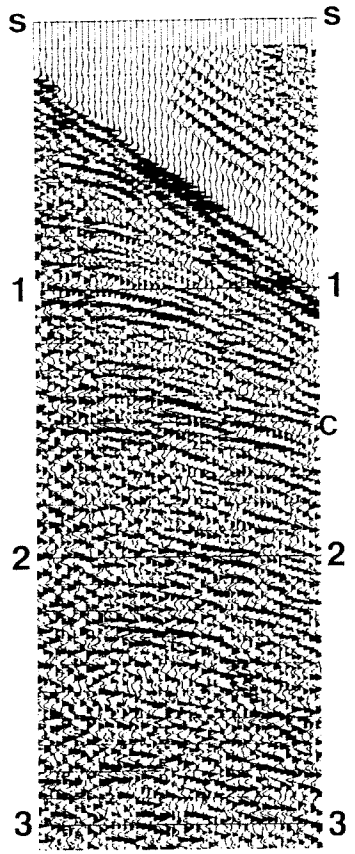

Figure 6.5 Common-shot gather with vibroseis source. Geometric spreading correction and trace balancing have been applied. Please note the two time scales in these different traces: one is the length of energetic reflecting pulses and the other one is the time between reflectors.

tracing. The presence of a core has also been demonstrated by Oldham in 1906 using rays, just after the beginning of modern seismology, and the inner core was discovered by Lehmann in 1936 (Bolt, 1982) from ray tracing interpretation of travel-time arrivals. At the global and regional scales, ray tracing is used in daily earthquake locations, in polarizations studies and in tomographic pictures of the Earth interior. Seismic profiles for oil research – diagram x^2-t^2, normal move-out, deep move-out, reflection hyperbole (Sheriff and Geldart, 1983a,b; Yilmaz, 1987) – exploit in an every day practical approach ray tracing results. Reflection tomography and migration techniques are techniques often based on ray theory.

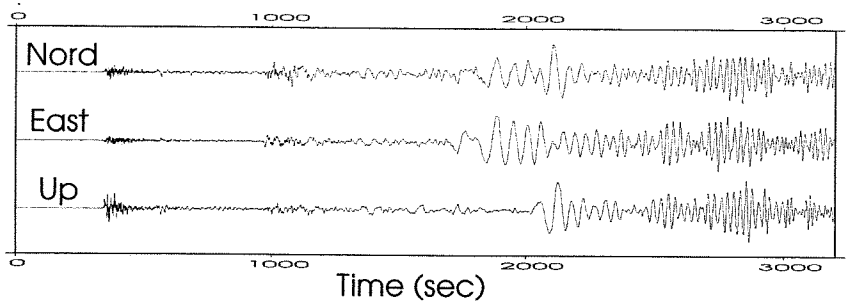

Figure 6.6 A broadband record of a major earthquake occurring the 4 October 1994 and recorded on new seismological instruments (TGRS network in the South of France) with a broad flat response between 50 Hz and 100 s. One can notice that this seismogram can be interpreted in different phases as P waves, S waves, Love waves, Rayleigh waves.

This rather lengthy introduction shows, hopefully, that understanding the ray theory is worth the required intellectual effort. Arguments in this lecture will show that seismology is an area where sophisticated tools based on ray theory have been designed for specific applications with no direct equivalence in other fields of physics. Acoustic wave propagation in oceans (Wunsch, 1987) have different ranges of approximation, electromagnetic propagation in the ionosphere (Wait, 1981) assumes with good accuracy layer approximation while optical ray tracing (Born and Wolf, 1986) is often made in homogeneous media. For ray tracing inside the Earth, we are on our own.

6.2 Wave propagation

In order to insert ray theory into the global frame of wave propagation, we shall introduce shortly wave propagation equations. Let us consider an heterogeneous elastic linear medium and a displacement $\mathbf{u}$ at a point M of cartesian coordinates (x, y, z). One can define two tensors of order 2 which can be written as a matrix at M: the stress tensor σ and the strain tensor ϵ. These infinitesimal tensors are local. The strain tensor is expressed with the help of the displacement vector of the point M. In a cartesian coordinate system, the expression

$$\epsilon_{ij} = \frac{1}{2}(u_{i,j} + u_{j,i}) \tag{6.1}$$

defines this relation. The comma in the subscripts indicates a partial derivative with respect to the associated following coordinate. The stress tensor which represents internal forces used in the elastodynamic equation

$$\sigma_{ij,j} + f_i = \rho u_{i,tt}, \tag{6.2}$$

with body forces f_i acting on point M. The stress tensor is related to the acceleration on the point M. The quantity ρ is the volumetric density. An additional relation is needed in order to connect the stress and the deformation. This relation defines the rheological behaviour of the material and is often the simple linear relation known as the Hooke law:

$$\sigma_{ij} = c_{ijkl}\,\epsilon_{kl} \tag{6.3}$$

where c_{ijkl} are elastic coefficients. Because of symmetrical relations, these 81 coefficients reduce to 21 independent ones. We find the linear elastodynamic equations under a general form for an anisotropic medium:

$$[c_{ijkl}u_{k,l}]_{,j} + f_i = \rho u_{i,tt} \tag{6.4}$$

where we shall admit that functions c_{ijkl} are differentiable and continuous, as well as its first derivative for our ray tracing presentation. The second derivative must exist and be continuous by step. We shall assume the same thing for the volumetric density. We shall see that these hypothesis are not too restrictive for high frequency approximation.

For an isotropic, linearly elastic body, the elastic coefficients can be expressed with only two independent ones as the Lamé parameters λ and μ for example:

$$c_{ijkl} = \lambda\delta_{ij}\delta_{kl} + \mu(\delta_{ik}\delta_{jl} + \delta_{il}\delta_{jk}). \tag{6.5}$$

Other choices are possible as the Young's modulus E or the Poisson coefficient ν or any linear expression well-adapted to the problem at hand. In an isotropic medium, we obtain the following elastodynamic linear equation (Aki and Richards, 1980):

$$(\lambda+\mu)u_{j,ij} + \mu u_{i,jj} + \lambda_{,i}u_{j,j} + \mu_{,j}[u_{i,j} + u_{j,i}] + f_i = \rho u_{i,tt}. \tag{6.6}$$

A further simplification is possible for material, such as water, where only compression takes place an shearing is not possible. There is only one independent parameter and the incompressibility modulus K at M is often the most suited one. The pressure variation P verifies the scalar equation:

$$\frac{1}{K(\mathbf{x})}P_{,tt}(\mathbf{x}, t) - \left(\frac{1}{\rho(\mathbf{x})}P_{,i}\right)_{,i}(\mathbf{x}, t) = S(\mathbf{x}, t) \tag{6.7}$$

where S is an explosive source with a pressure variation in space and in time. For a homogeneous volumetric density, we simply obtain the wave equation:

$$\Delta P(\mathbf{x}, t) - \frac{1}{c^2(\mathbf{x})}P_{,tt}(\mathbf{x}, t) = -S(\mathbf{x}, t) \tag{6.8}$$

where Δ denotes the laplacian at the point M and c is the wave speed.

Terminology is rather confusing between the wave equation, the scalar wave equation, the vectorial wave equation, the acoustic wave equation, the elastodynamic equation. For my point of view, the wave equation involves only the displacement while the elastodynamic equation takes into account the stress as well. To be aware of this slight ambiguity about the vocabulary is the best way to solve the difficulty often met with these equations.

Before closing the section, presenting the solution of the wave equation in a homogeneous medium is interesting for the ray theory later on. One can say that such a simple example does not require a complete discussion. As far as I know, obtaining this solution is difficult, requiring a careful analysis of opposite singularities at the source position: it is far from obvious (Morse and Feshbach, 1953, p. 834; Bleistein, 1984).

Let us first consider a laplacian of a scalar quantity g which is singular inside a small volume of radius ϵ around the source. The singularity is such that the point source is impulsive, *i.e.*

$$\iiint \Delta g(r)\, dv \to -\iiint \delta(\mathbf{x})\, dv = -1, \tag{6.9}$$

as the volume of integration shrinks to zero. We apply the Gauss theorem for reducing the volume integral down to a surface integral and then we take into account the symmetry of the geometry to evaluate the surface integral. We find the following equations

$$\iiint \Delta g(r)\, dv = \iint \mathbf{grad}(g) \cdot \mathbf{dS}, \tag{6.10}$$

$$\iiint \Delta g(r)\, dv = 4\pi\epsilon^2 \left(\frac{dg}{dr}\right)_{r=\epsilon}. \tag{6.11}$$

By comparison with eq. (6.9), we find that the term dg/dr behaves as $-1/r^2$ and, consequently, that the scalar quantity g behaves as $1/r$ when r goes to zero.

For the acoustic wave equation in a three-dimensional homogeneous medium with an impulsive point source,

$$\Delta P(\mathbf{x}, t) - 1/c^2 P_{,tt}(\mathbf{x}, t) = -\delta(\mathbf{x})\, \delta(t) \tag{6.12}$$

an heuristic argument is to consider the laplacian as the dominant term compared to the time derivative since the laplacian involves the second derivatives of a three-dimensional function $\delta(\mathbf{x})$. The function $\delta(\mathbf{x})$ includes the product of three singular functions. A more rigorous approach can be found in Morse and Fechbach (1953, p. 838), although the final conclusion will leave us with only the laplacian term as the singular term in the eq. (6.12). Taking also into account the result of the eq. (6.11), the behaviour of P would be when r goes to zero

$$P(r, t) \to \delta(t)/4\pi r. \tag{6.13}$$

We look for a solution of the eq. (6.12) without the left hand side which verifies this condition (6.13). Because the medium is homogeneous and the source has a spherical symmetry, the pressure field P will only depend on the radius r. The expression of the laplacian in spherical coordinates gives:

$$1/r^2 \frac{\partial}{\partial r}\left(r^2 \frac{\partial P}{\partial r}\right) - 1/c^2 \frac{\partial^2 P}{\partial t^2} = 0 \tag{6.14}$$

which reduces to the equation

$$\frac{\partial^2 (Pr)}{\partial r^2} - 1/c^2 \frac{\partial^2 (Pr)}{\partial t^2} = 0, \tag{6.15}$$

the fundamental solution P of which is composed of two arbitrary functions h and k in the following expression:

$$P(r, t) = [h(t - r/c) + k(t + r/c)]/r. \tag{6.16}$$

From the condition (6.13), only the functions $\delta(t-r/c)/r$ or $\delta(t+r/c)/r$ are allowed as well as any combination of these two quantities. The second solution can be eliminated because the impulse given at time zero must be felt at the position r only later on. The elementary solution in a three-dimensional homogeneous medium

$$P(r, t) = \frac{1}{4\pi}\, \delta(t - r/c)/r \tag{6.17}$$

is the impulsive function weighted with a geometrical decrease $1/r$. This perturbation propagates at speed c as damped concentric shells. For a general source $S(\mathbf{r}_0, t)$, we consider the convolution product of an impulsive function with the source function and we find the well-known function G called delayed potential in physics

$$G(\mathbf{r}, t) = \frac{1}{4\pi} \int_{V_0} dv_0 \frac{S(\mathbf{r}_0, t - R/c)}{R}, \tag{6.18}$$

where R is the distance between the point $\mathbf{r}$ and the integration point $\mathbf{r}_0$ over the source zone V_0.

For the two-dimensional case where the distribution of sources is along the y axis, an integration of the solution (6.17) along this axis gives the following elementary solution with respect to the cylindrical distance r' from the source

$$P(r', t) = \frac{1}{2\pi} \frac{H(t - r'/c)}{\sqrt{(t^2 - r'^2/c^2)}}, \tag{6.19}$$

with a typical tail after the wavefront, well pictured by Bleistein (1984, p. 64) for flatland residents. $H(t)$ is the heaviside function which is zero for negative t and one for positive t. By another integration of the eq. (6.19) along the z axis, one can deduce the elementary solution for an one-dimensional medium along the x axis:

$$P(x, t) = \frac{c}{2} H(t - x/c). \tag{6.20}$$

A given point stays at rest until it is reached by a constant pressure at time $t-x/c$. The time derivative of the pressure may be a better quantity with an impulsive shape. By anticipating on the definition of the Fourier transformation, we must underline that the solution (6.17) has the following Fourier transformation with respect to time

$$\frac{1}{4\pi r} e^{i\omega r/c}, \tag{6.21}$$

while the Fourier transformation of the two-dimensional solution (6.19) is the

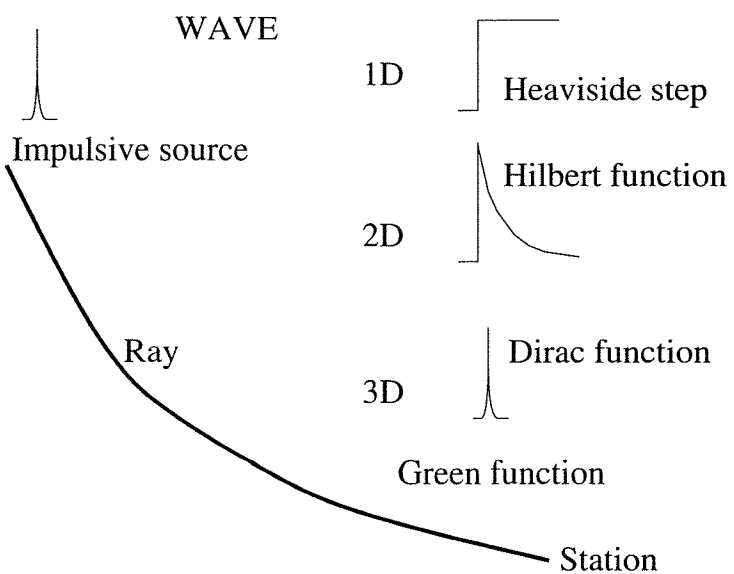

Figure 6.7 Typical shape of the Green function in a homogeneous medium. Only the dimension of the space is changing, as well as the source excitation. For a 1D medium, the excitation is from a plane wave. For a 2D medium, the excitation is from a line source. For a 3D medium, the excitation is from a point source. Please, note the slowly decaying part for the 2D Green function.

Bessel function singular at the origin, *i.e.* the Hankel function of order zero:

$$\frac{i}{4} H_0^1(\omega r'/c). \tag{6.22}$$

Finally, the Fourier transformation of the derivative of the pressure for an one-dimensional medium is

$$\frac{1}{4\pi} e^{i\omega x/c}. \tag{6.23}$$

These solutions (Figure 6.7) are very important for the normalization of the asymptotic solutions of the ray theory. Their construction is far from obvious, but these solutions which have a wide importance in physics will be quite natural and intuitive to the reader after a while.

6.3 How to solve wave equations

Construction of solutions for the wave equation or the elastodynamic equation is a difficult task. In these notes, a schematic description will be performed in order to situate the ray theory among them in a global frame.

One can consider three main groups of methods with possible bridges between particular approaches.

6.3.1 *Space methods*

The first approach deals with the space $(\mathbf{x}, t)$ where numerical methods solve directly the partial differential equations of wave theory. Finite difference (Alterman and Karal, 1968; Kelly *et al.*, 1976; Virieux, 1984,1986 among others) or finite element (Lysmer and Drake, 1972; Badal and Serón, 1986) methods are brute force methods and are very well suited to computers with specific hardware architecture as vectorized pipelines or SIMD (single instruction and multiple data) machines. Variations in order to estimate partial derivatives are based on interpolating functions: Fourier methods, also called pseudo-spectral methods, go to the Fourier domain in order to evaluate partial derivatives (Kosloff and Baysal, 1982; Kosloff *et al.*, 1984), while differential equations are still verified in the space domain $(\mathbf{x}, t)$. Let us underline that spectral methods we are going to see in paragraph 6.3.2 verify equations and boundary conditions in the Fourier domain. Integral equations in real space (Brebbia, 1984; Bonnet, 1986; Hirose and Achenbach, 1989) are also an alternative to the resolution of differential equations. These integral equations have the advantage of reducing by one dimension the problem to be solved at the expense of a linear system with full matrices while the finite element method deals often with sparse matrices.

6.3.2 *Spectral methods*

The second group manages a transformation towards a new space $(\mathbf{k}, \omega)$, where the resolution of the transformed equations are expected to be simpler. These methods, called spectral methods, have many variations as the reflectivity method (Fuchs and Müller, 1971), discrete wave number method (Bouchon and Aki, 1977; Bouchon *et al.*, 1989), slowness methods (Chapman, 1978) or integral equations (Brebbia, 1978) and a mixture of these different approaches (Campillo, 1987; Gaffet and Bouchon, 1989). Depending on the spatial variations of the medium properties, the separation of partial derivatives will be partial or complete. For partial separation, one can select the space $(\mathbf{x}, t)$ in the unsolved direction and use previous methods in order to obtain the solution (Alekseev and Mikhailenko, 1980). Transformation back to the real space are always required at the final stage.

The major disadvantage of the two already mentioned groups is a great difficulty for the interpretation of synthetic seismograms. For the first kind of methods in the space domain, only time snapshots of the medium allow to identify phases. This interpretation can be a very cumbersome task, while the situation is even worse for spectral method where one can check the validity of the solution only when the solution comes back to real space.

6.3.3 *Asymptotic methods*

A third class of methods assumes an asymptotic behaviour at high frequency as the ray theory (Červený *et al.*, 1977), the WKBJ method (Chapman, 1978) for stratified media or the Maslov method (Chapman and Drummond, 1982; Chapman, 1985; Thomson and Chapman, 1985) available for laterally varying media. Techniques of beam summations such as the gaussian beam summation GBS (Popov, 1982; Červený *et al.*, 1982; Weber, 1988) have increased the interest of the seismological community in these asymptotic methods. The main advantage of these methods is not only their computer efficiency but their capacity of physical interpretation of computed results. Asymptotic approach constructs only a part of the solution as direct *P* wave or reflected *PS* wave, making the identification and the interpretation of this phase very simple.

6.4 Scalar high frequency approximation

We want to construct a high frequency approximation of the solution of the wave equation and, in order to do so, we start from an assumed expression of its Fourier transformation. At high frequency, this expression is related to the wavefront notion which is not destroyed by the heterogeneity of the medium. The use of the Fourier transformation is not strictly necessary as long as the wavefront meaning is kept (see, for example, Keilis-Borok *et al.*, 1989, for a space-time presentation). We shall not discuss this space-time ray theory in these notes.

6.4.1 *Ansatz of the ray theory*

For the introduction of the high frequency approximation, we need a definition of the Fourier transformation of the function f and we assume the following expression:

$$f(\omega) = \int_{-\infty}^{+\infty} f(t)\, e^{i\omega t}\, dt, \tag{6.24}$$

with the inverse transformation

$$f(t) = \frac{1}{2\pi} \int_{-\infty}^{+\infty} f(\omega)\, e^{-i\omega t}\, d\omega. \tag{6.25}$$

We shall keep the same notation for the function and its transformation: the argument of the function will tell us in which space we are. Let us recall the acoustic wave equation:

$$\nabla^2 P(\mathbf{x}, t) - \frac{1}{c^2(\mathbf{x})} \frac{\partial^2 P(\mathbf{x}, t)}{\partial t^2} = -S(\mathbf{x}, t), \tag{6.26}$$

where P is the pressure in $\mathbf{x}$ at time t and S is the source function. The propagation velocity $c(\mathbf{x})$ may vary continuously in space. Initial conditions are requested and a zero pressure is the simplest condition as well as a zero temporal derivative in every point of the space at time zero. In the frequency domain, the wave equation becomes the Helmholtz equation:

$$\nabla^2 P(\mathbf{x}, \omega) + \frac{\omega^2}{c^2(\mathbf{x})} P(\mathbf{x}, \omega) = 0, \tag{6.27}$$

outside the source area. The wave number is denoted by $k = \omega/c$. The solution of this equation may be rather complex, but physical considerations allow us to assume a particular form of the solution. An intuitive argument comes from the solution in a three-dimensional homogeneous space

$$\frac{1}{4\pi r} e^{i\omega T}, \tag{6.28}$$

with two distinct terms: the first one defines the amplitude while the second locates the wavefront. The travel-time T is r/c in a homogeneous medium. The coherence of the wave front might be preserved in heterogeneous media with a travel-time and an amplitude defined locally. Wave fronts are deformed but still

exists. Figure 6.8 shows an example on the left where wavefronts are still visible in spite of the heterogeneity of the medium and an example on the right where the heterogeneity variation destroy entirely the wavefront coherence. Formally, the ansatz of the solution will be:

$$P(\mathbf{x}, \omega) = S(\omega) A(\mathbf{x}, \omega) e^{i\omega T(\mathbf{x})} \tag{6.29}$$

where the function $S(\omega)$ is defined by initial conditions (source description or boundary excitation, for example...). The asymptotic approximation assumes that the function $A(\mathbf{x}, \omega)$ has the following form:

$$A(\mathbf{x}, \omega) = \sum_{k=0}^{k=\infty} \frac{A_k(\mathbf{x})}{(-i\omega)^k}, \tag{6.30}$$

which splits the spatial dependence and the frequential or temporal dependence. From the practical point of view, we are interested only in the zero-order approximation, *i.e.* $A(\mathbf{x}, \omega) = A_0(\mathbf{x})$. The zero-order solution becomes

$$P(\mathbf{x}, \omega) = S(\omega) A_0(\mathbf{x}) e^{i\omega T(\mathbf{x})}. \tag{6.31}$$

In the time domain, the solution has an elegant analytical time dependence

$$P(\mathbf{x}, t) = A_0(\mathbf{x}) S(t - T), \tag{6.32}$$

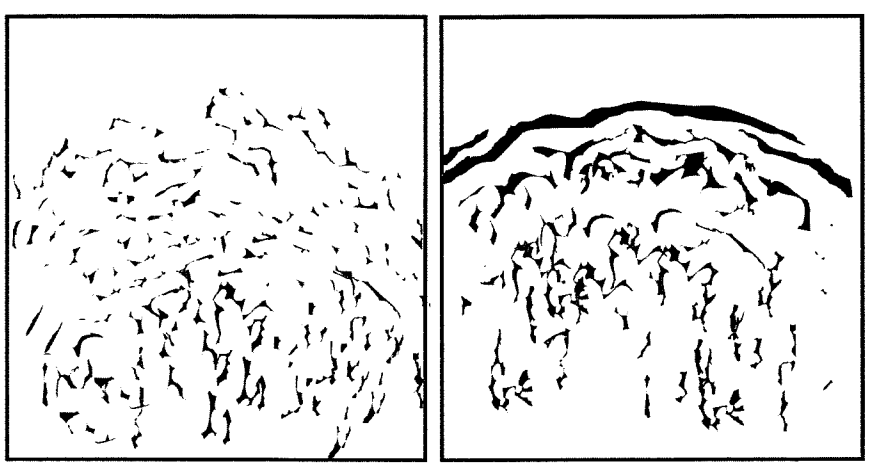

Figure 6.8 On the right panel, initial wavefronts are still present, while on the left panel the initial wavefronts are completely disorganized.

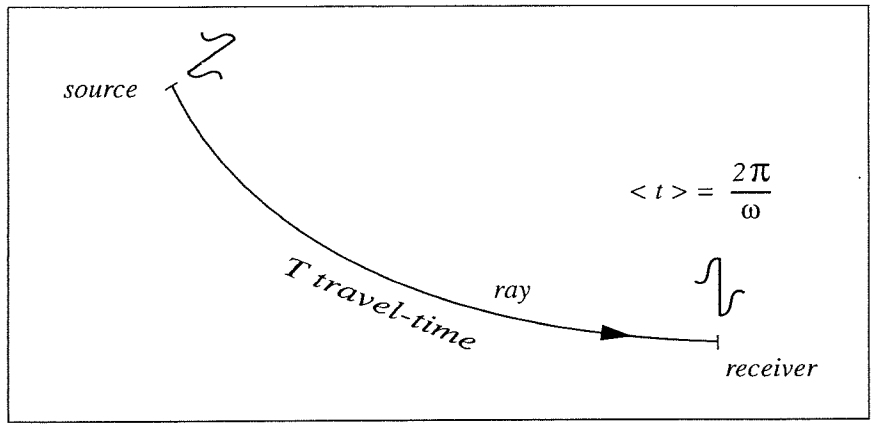

Figure 6.9 Schematic diagram with travel-time scale T and source time scale defined by $<t>$.

which demonstrates that the source signal S propagates without distortion at high frequency with a travel-time T. We shall assume that the source function spectra is zero for frequencies lower than ω_m. Moreover, we consider only positive frequencies. We shall see later on how to take into account negative frequencies (Chapman, 1978).

We have now the explicit demonstration of two time scales in the seismic signal: the travel-time T and the characteristic time of the source $<t>$ as shown in Figure 6.9. This time of the source defines the spectral bandwidth of the emitted energy by the relation $<t> = 2\pi/\omega$ and the high-frequency approximation will be valid if $\omega T >> 1$. If this is not the case, we have interferences betweeen the propagated source signal and the medium. Diffraction and distortion effects happen and additional terms of the series (6.30) might partially model these effects at the expense of additional difficulties (Červený and Ravindra, 1971; Chapman and Coates, 1994).

One must underline that exact solutions for a point source in three-dimensional and one-dimensional homogeneous media have the correct expression for the ray theory where the signal propagates without deformation. For the two-dimensional case, the exact solution is not a delayed potential: we must look for its high frequency approximation. Going through the Fourier transform, which is the Hankel function of zero order H_0^1, one might write the asymptotic form of H_0^1, which is a plane wave

$$P(r, \omega) = \frac{i}{4} H_0^1(\omega r/c) \simeq \frac{i}{4} \sqrt{\frac{2c}{\pi \omega r}} e^{i\omega r/c} e^{-i\pi/4}. \tag{6.33}$$

This plane wave has a compatible form with the ray theory:

$$P(r,\,\omega) = \left[\frac{1}{4\pi}\sqrt{\pi/\omega}\,e^{i\pi/4}\right]\left[\sqrt{2\frac{c}{r}}\right]e^{i\omega r/c}. \tag{6.34}$$

The final approximation in time domain can be written as

$$P(r,\,t) = \frac{1}{2\pi}\sqrt{c/2r}\,\frac{H(t-r/c)}{\sqrt{t-r/c}} \tag{6.35}$$

which is a good approximation of the exact solution near the wave front where the time can be estimated to r/c in the following expression

$$\sqrt{t^2-\frac{r^2}{c^2}} \simeq \sqrt{2r/c}\sqrt{t-\frac{r}{c}}\,. \tag{6.36}$$

Let us go back to the asymptotic series. Inserting the ansatz (6.29) as well as the series (6.30) in the Helmholtz eq. (6.27) and ordering terms in power of the frequency ω, we find with the help of the two following equalities:

$$\nabla P = (\nabla A e^{i\omega T} + i\omega \nabla T A e^{i\omega T}) \tag{6.37}$$

$$\nabla^2 P = (\nabla^2 A e^{i\omega T} + i\omega[2\nabla A\cdot\nabla T + A\nabla^2 T]e^{i\omega T} - \omega^2(\nabla T)^2 A e^{i\omega T}) \tag{6.38}$$

the cascade of equations

$$\text{in } \omega^2 : ((\nabla T)^2 - 1/c^2)A_0 = 0$$

$$\text{in } -i\omega : (2\nabla A_0 \nabla T + \nabla^2 T A_0) = 0$$

$$\text{in } (-i\omega)^{-k} : \nabla^2 A_k + 2\nabla A_{k+1}\nabla T + (\nabla T)^2 A_{k+1}) = 0 \quad \text{for } k > 0\,.$$

The equations for the two first powers of ω attract our attention. The first equation, called eikonal (from picture in greek),

$$(\nabla T)^2 = \frac{1}{c^2}\,, \tag{6.39}$$

takes into account only the travel-time, while the second equation

$$2\nabla A_0 \cdot \nabla T + \nabla^2 T A_0 = 0\,, \tag{6.40}$$

allows computation or transport of the amplitude at time T. We call it the transport equation. The other equations allow formal estimation of higher terms in the series.

The convergence of the series is not analyzed. We only need a formal identity with the wave equation: higher terms can be far from negligable quantities, as for critical reflections, creeping waves and some conversions of compressive waves into shearing waves (Weber, 1988; Thomson, 1989; Yedlin *et al.*, 1990).

6.4.2 *Eikonal equation*

The eikonal equation

$$(\nabla T(\mathbf{x}))^2 - \frac{1}{c^2(\mathbf{x})} = 0\,, \tag{6.41}$$

is the basic equation which controls the evolution of wavefronts. We shall see that it is also true in elastic media for each kind of wave. Solving this equation is related to the kinematic propagation of wavefronts defined by equal phase surface $T(\mathbf{x}) = T_0$. Looking for the evolution of the function $T(\mathbf{x})$ can be performed in complex media where the high frequency approximation looses its meaning: wavefronts exist even when a medium has rapid variations. One can construct wavefronts at time $t+dt$ knowing the wave front at time t: it is enough to use the Huyghens principle for the geometrical construction. A constant length is taken away for the initial wave front such that the modulus of the gradient ∇T is equal to $1/c(\mathbf{x})$ at the current point as shown graphically (Figure 6.10). This technique has been extensively exploited in a graphical approach of the wave propagation (Riznichenko, 1946) and for graphical interpretation of refracted profiles (Figure 6.11). Because computer memory has become rather inexpensive this method, which requires important memory capacities, is now an attractive alternative to ray tracing for specific applications. Its computer implementation solves the eikonal equation by finite differences on a regular grid for the first travel-time (Vidale,

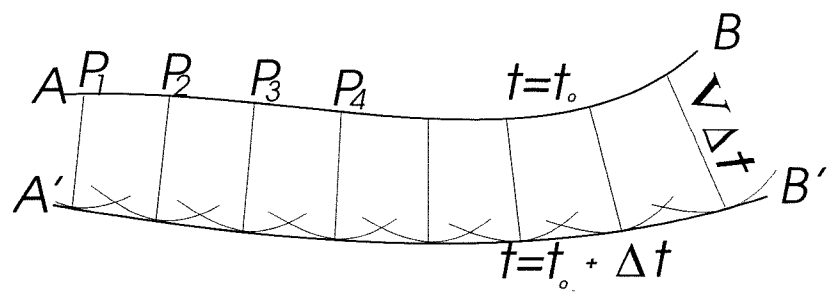

Figure 6.10 Construction of a new wavefront at time $t_0+\Delta t$ from the wavefront at time t_0. The length perpendicular to the wavefront is proportional to the speed V times the time increment.

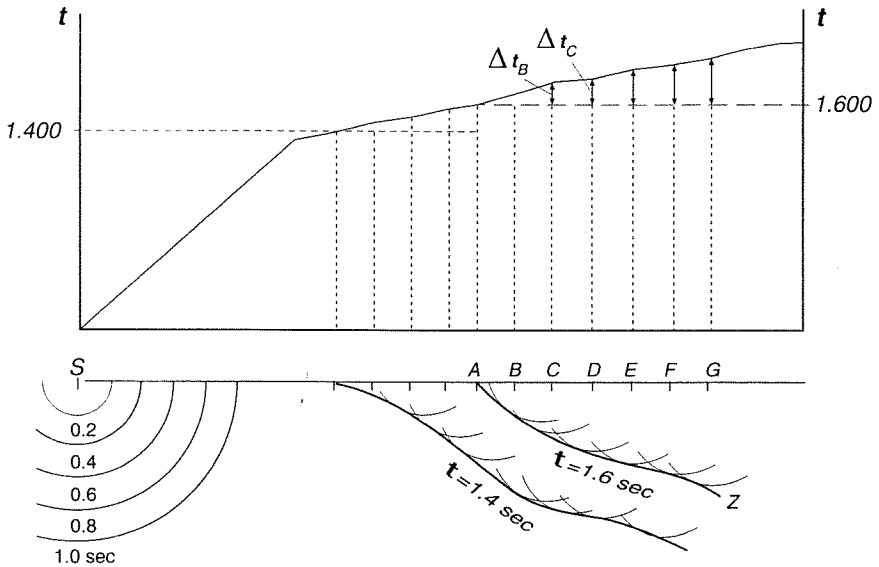

Figure 6.11 Reconstruction of wavefronts from refracted profils after *Applied Geophysics* by Telford *et al.* (1976). From travel times observed, one can project back into the medium wavefront for time equal to 1.6 s corresponding to point A. It is possible to start again for another wavefront at 1.4 s for example.

1988; Moser, 1991; Podvin and Lecomte, 1991; Klimeš and Kvasnička, 1994, among others). Applications of these methods for locating earthquakes have been published (Moser *et al.*, 1992; Wittlinger *et al.*, 1993) while we are still waiting for tomographic applications of this wavefront propagation. An obvious feature of these approaches is the necessity of sampling the whole medium while ray tracing will only sample a line inside the medium. Consequently, ray theory is and will be an efficient tool in seismology even if sampling the entire medium is sometimes required for some applications.

Instead of looking for wavefronts, we might focus our attention on orthogonal trajectories to wavefronts at each point (Figure 6.12). These trajectories are rays which have not the obvious physical support that they have in optics. The morphologic structure of our eye is responsible of this fact. Tracing rays, instead of wavefronts, is the standard way to solve ordinary differential equations, an approach we are going to set up. This approach is called the characteristic method. Let us consider the implicit equation of a ray $\mathbf{x}(s)$ where s is the curvilinear abscisse. The tangent is defined by

$$\mathbf{t} = \frac{d\mathbf{x}}{ds} \tag{6.42}$$

with a modulus equal to one by definition of the curvilinear abscissa. From the ray definition as an orthogonal trajectory, the tangent is parallel to ∇T. From the eikonal equation, one can deduce the following equation

$$\frac{d\mathbf{x}}{ds} = c\nabla T. \tag{6.43}$$

We often say that $|\,d\mathbf{x}\,|/c$ is the optical distance. After this tangent evolution of rays, we must study the normal evolution which comes with the evaluation of

$$\frac{d\nabla T}{ds} = \frac{d}{ds}\left(\frac{1}{c}\frac{d\mathbf{x}}{ds}\right). \tag{6.44}$$

Knowing that the derivative with respect to the curvilinear abscissa s is the projection of the vectorial gradient on the tangent $\mathbf{t}$, we obtain the following operator applied to each component of a vectorial quantity:

$$\frac{d}{ds} = \mathbf{t}\cdot\nabla = c\nabla T\cdot\nabla, \tag{6.45}$$

where we use the operator notation for vectorial gradient. We have successively

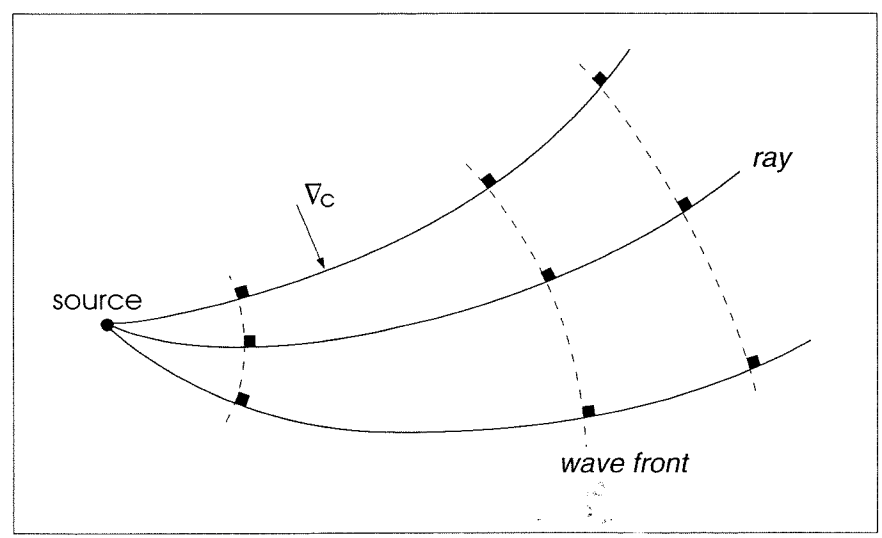

Figure 6.12 Rays are orthogonal trajectories to wavefronts.

and formally the following equalities

$$\frac{d\nabla T}{ds} = c\nabla T \cdot \nabla(\nabla \mathbf{T})$$
$$\frac{d\nabla T}{ds} = \frac{c}{2}\nabla(\nabla T)^2$$
$$\frac{d\nabla T}{ds} = \frac{c}{2}\nabla\left(\frac{1}{c}\right)^2$$
$$\frac{d\nabla T}{ds} = \nabla\left(\frac{1}{c}\right) \tag{6.46}$$

from which we can deduce, with the help of eq. (6.44), the equation describing the evolution of the normal part of ray trajectories

$$\frac{d}{ds}\left(\frac{1}{c}\frac{d\mathbf{x}}{ds}\right) = \nabla\left(\frac{1}{c}\right). \tag{6.47}$$

This equation is also called the curvature equation because differentiation implies

$$\nabla\left(\frac{1}{c}\right) = \mathbf{t}\frac{d}{ds}\left(\frac{1}{c}\right) + \frac{1}{c}\frac{d\mathbf{t}}{ds} \tag{6.48}$$

and, using the definition of curvature $\mathcal{K}$ in the Frénet system as mentioned in Figure 6.13

$$\frac{d\mathbf{t}}{ds} = \mathcal{K}\mathbf{n}, \tag{6.49}$$

we find

$$\nabla\left(\frac{1}{c}\right) = \mathbf{t}\frac{d}{ds}\left(\frac{1}{c}\right) + \frac{\mathcal{K}}{c}\mathbf{n}. \tag{6.50}$$

This relation is better written explicitly with the slowness $u = 1/c$,

$$\nabla u = \mathbf{t}\frac{du}{ds} + \mathcal{K}u\mathbf{n}. \tag{6.51}$$

The scalar product of this equation with the normal **n** controls the evolution of

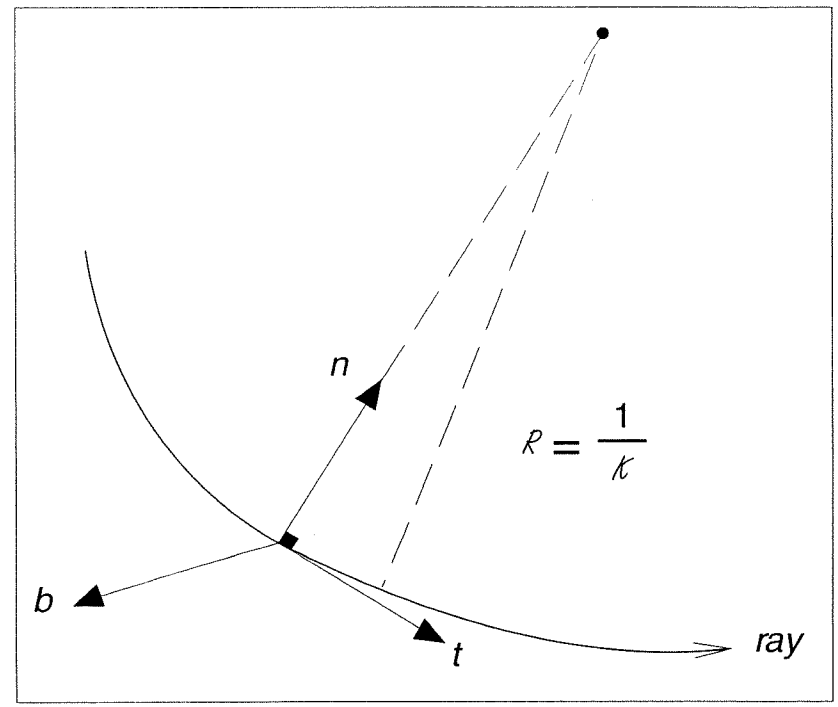

Figure 6.13 Frénet system (**t**, **n**, **b**) with curvature $\mathcal{K}$. The torsion $\mathcal{T}$ will define the rotation of this frame as we move along the ray (see Figure 6.15).

the curvature, which gives explicitly

$$\begin{aligned}\mathcal{K} &= 1/u\,\mathbf{n}\cdot\nabla\mathbf{u}\\ &= 1/u\,\partial u/\partial n\\ &= -1/c\,\partial c/\partial n.\end{aligned} \tag{6.52}$$

The curvature increases in the opposite direction of the velocity gradient perpendicular to the ray. Figure 6.14 indicates the vectorial construction deduced from eq. (6.51) and allows the introduction of the angle i between the gradient of the slowness and the tangent to the ray with the simple relation

$$\mathcal{K} = \frac{1}{u}|\nabla u|\,\sin i. \tag{6.53}$$

The torsion $\mathcal{T}$ is defined as the scalar product between $d\mathbf{n}/ds$ and the binormal **b**.

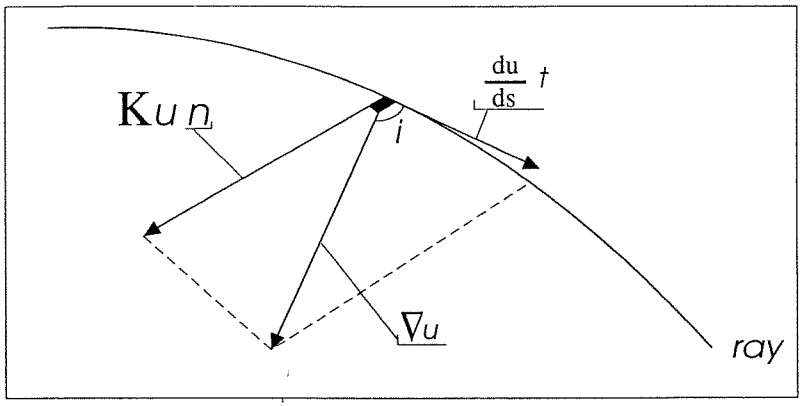

Figure 6.14 Geometrical interpretation of ray tracing equation: rays are bent towards the gradient of the slowness u.

From the expression of the normal

$$\mathbf{n} = \frac{1}{\mathcal{K}u}\left[-\frac{du}{ds}\mathbf{t} + \nabla u\right], \tag{6.54}$$

one can deduce that the only contribution to the derivative of $\mathbf{n}$ with respect to the curvilinear abscissa s along the binormal comes from the following term

$$\frac{1}{\mathcal{K}u}\frac{d\nabla u}{ds}. \tag{6.55}$$

The torsion $\mathcal{T}$ interpreted in Figure 6.15 given by

$$\mathcal{T} = \frac{1}{\mathcal{K}u}\frac{d\nabla u}{ds}\cdot\mathbf{b}$$

$$\mathcal{T} = -\frac{1}{\mathcal{K}c}\frac{d\nabla c}{ds}\cdot\mathbf{b} \tag{6.56}$$

is essential for the elastic case to estimate the evolution of the polarization. For the moment, it completes the geometrical analysis of ray tracing. After these considerations, we may trace rays with the help of the curvature eq. (6.47) which is a non-linear second-order vector ordinary differential equation (non-linear O.D.E).

It is natural to reduce the order of the differential system by introducing an additional variable which comes from the equation along the tangent. This variable, called slowness vector $\mathbf{p}$, is defined by

$$\mathbf{p} = \nabla T = \frac{1}{c}\frac{d\mathbf{x}}{ds}. \tag{6.57}$$

An important system of first-order differential equations is deduced

$$\frac{d\mathbf{x}}{ds} = c\,\mathbf{p}$$

$$\frac{d\mathbf{p}}{ds} = \nabla\left(\frac{1}{c}\right) \tag{6.58}$$

with the following constraint coming from the eikonal equation

$$|p| = \frac{1}{c}. \tag{6.59}$$

The phase or travel-time is obtained by integration of the eikonal equation along the ray, *i.e.*

$$\frac{dT}{ds} = \frac{1}{c} = u. \tag{6.60}$$

We shall study the coupled non-linear system (6.58) where the velocity c depends on position $\mathbf{x}$ instead of the non-linear eq. (6.47) because the variable $\mathbf{p}$ not only plays the role of an auxiliary variable but has a physical interpretation as important as the position meaning. We might expect behaviours of O.D.Es with the influence of initial conditions, with the geometrical structure of the solution coming from the catastrophe theory, with stiffness, strange attractors and so on (Gilmore, 1981). This problem in itself is a difficult problem to solve and we shall spend part of our effort in order to analyze it. Before doing so, we shall examine the transport equation.

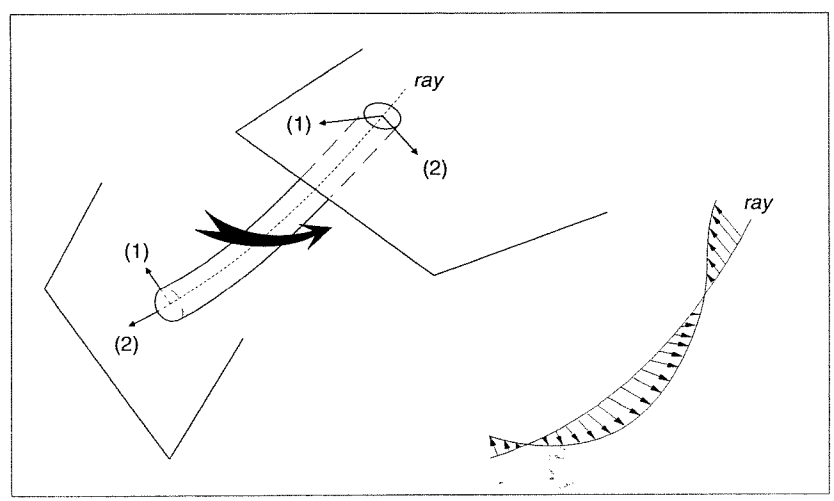

Figure 6.15 Two schematic diagrams for geometrical interpretation of torsion $\mathcal{T}$.

6.4.3 *Transport equation*

The transport equation, which is written

$$2\nabla A_0 \nabla \mathbf{T} + \nabla^2 T A_0 = 0\,, \tag{6.61}$$

might be converted into a simpler form by multiplying the eq. (6.61) with the non-zero quantity A_0 in order to get a divergence

$$\text{div}\ (A_0^2 \nabla \mathbf{T}) = 0\,. \tag{6.62}$$

Around a ray, let us consider an elementary cylindrical tube of volume V with a generatrix parallel to a segment of ray. The intersected surface by the cylindrical tube is described by two parameters γ_1 and γ_2 (Figure 6.16) such that the elementary surface is:

$$\mathbf{dS} = dS\mathbf{n} = \left(\frac{\partial \mathbf{x}}{\partial \gamma_1} \times \frac{\partial \mathbf{x}}{\partial \gamma_2}\right) d\gamma_1\, d\gamma_2\,. \tag{6.63}$$

The cross product is denoted by $\times$. The two elementary surfaces at curvilinear abscissa s_0 and s_1 are denoted by dS_0 and dS_1. The use of the divergence theorem permits us to write

$$\int\int\int \text{div}\,(A_0^2 \nabla \mathbf{T})\, dv = \int\int A_0^2\, \mathbf{n} \cdot \nabla \mathbf{T} dS = 0\,, \tag{6.64}$$

which means that the flux of the field $A_0^2 \nabla \mathbf{T}$ is preserved during the propagation. Only the flux across the two surfaces dS_0 and dS_1 exists. Knowing that $\nabla \mathbf{T}$ is parallel to $\mathbf{p}$, we can introduce two new surfaces dS'_0 and dS'_1, projections of surfaces dS_0 and dS_1 on the normal to the ray (Figure 6.16). We obtain the following equality

$$\frac{1}{c_0} A_0^2\,(s_0)\, dS'_0 = \frac{1}{c_1} A_0^2\,(s_1)\, dS'_1 \tag{6.65}$$

where we have introduced the slowness u_0 and u_1 at positions s_0 and s_1. This eq. (6.65) allows the amplitude computation at position s_1 from the amplitude at position s_0. This represents the energy flux averaged over a propagation time proportional to $1/c$ through the surface dS'. The zero-order approximation implies that the energy is preserved in the ray tube without any loss through lateral sides. We find

$$A_0\,(s_1) = A_0\,(s_0) \sqrt{\frac{c_1\, dS'}{c_0\, dS'_1}}\,. \tag{6.66}$$

The surface

$$dS' = dS\mathbf{n} \cdot \mathbf{t} = J\, d\gamma_1\, d\gamma_2 \tag{6.67}$$

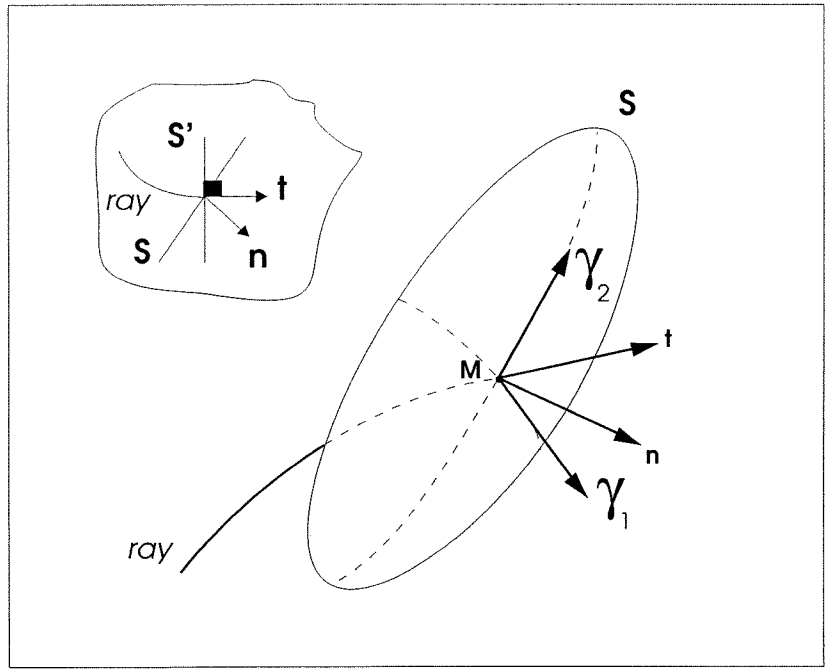

Figure 6.16 Parametrization of the surface S at the point M of the ray. The ray tube is supported by this surface S at each time t. The surface S' is required for amplitude estimation but it is not necessary for ray tracing.

is interpreted with the help of the jacobian

$$J = \begin{vmatrix} \dfrac{\partial x}{\partial s} & \dfrac{\partial x}{\partial \gamma_1} & \dfrac{\partial x}{\partial \gamma_2} \\ \dfrac{\partial y}{\partial s} & \dfrac{\partial y}{\partial \gamma_1} & \dfrac{\partial y}{\partial \gamma_2} \\ \dfrac{\partial z}{\partial s} & \dfrac{\partial z}{\partial \gamma_1} & \dfrac{\partial z}{\partial \gamma_2} \end{vmatrix} \tag{6.68}$$

noted also

$$J = \left| \frac{\partial\,(x,\, y,\, z)}{\partial\,(s,\, \gamma_1,\, \gamma_2)} \right| = (\mathbf{t},\, \gamma_1,\, \gamma_2)\,, \tag{6.69}$$

where vectors γ_1 and γ_2 are unitary vectors perpendicular to the tangente **t**. We obtain the generic formula for the acoustic case

$$A_0(s_1) = A_0(s_0)\sqrt{\frac{c_1 J_0}{c_0 J_1}} \tag{6.70}$$

which can also be written

$$A_0(s_1) = A_0(s_0)\sqrt{\frac{u_0 J_0}{u_1 J_1}}\,. \tag{6.71}$$

Often, one takes as elementary surfaces the surfaces S' only while we have more freedom to consider also surfaces S. We might be interested by surfaces S and not only S' during ray tracing. This subtle advantage has its importance in designing ray tracing programs. In any case, at the station point, we should go back to the surface S' in order to compute the amplitude. The use of arbitrary surfaces S is a freedom which makes easier the ray tracing with initial excitations on vibrating surfaces which are not wavefronts, interface projections... Of course, we have to go back to surfaces S' in order to determine the amplification modulation.

We are now able to describe the pressure observed at a given point coming from a source with temporal variation $S(\omega)$ and with a radiation pattern $\phi(\gamma_1, \gamma_2)$. One can distinguish the excitation, the geometrical spreading and the propagation:

$$P(x, \omega) = S(\omega)\,\phi(\gamma_1, \gamma_2)\sqrt{\frac{c}{J}}\,e^{i\omega T(\mathbf{x})}. \tag{6.72}$$

How to estimate the intensity of the source ϕ? A possible solution is to select a particular example as a homogeneous medium of speed c_0. We look at a canonical problem in order to calibrate the high frequency solution with an already known solution (Červený, 1985). At the source itself, a singularity must move away at a distance of at least a wavelength. The complete high frequency Green function is given by

$$P(r, \omega) = S(\omega)\frac{1}{4\pi}\frac{1}{r}\,e^{i\omega T}. \tag{6.73}$$

The jacobian is defined by $dS = J\,d\Omega$, which gives by integration on the sphere

$$4\pi R^2 = J\int d\Omega = 4\pi J\,. \tag{6.74}$$

We write the solution in the asymptotic form

$$P(r, \omega) = S(\omega)\frac{1}{4\omega\sqrt{c_0}}\sqrt{\frac{c_0}{J}}\,e^{i\omega T}, \tag{6.75}$$

that permits us to identify the radiation term of the isotropic and point source:

$$\phi(\gamma_1, \gamma_2) = \frac{1}{4\pi\sqrt{c_0}}\,. \tag{6.76}$$

We deduce the asymptotic solution for a variable velocity $c(\mathbf{x})$:

$$P(\mathbf{x}, \omega) = S(\omega)\frac{1}{4\pi\sqrt{c_0}}\sqrt{\frac{c(\mathbf{x})}{J(\mathbf{x})}}\,e^{i\omega T(\mathbf{x})}, \tag{6.77}$$

where c_0 is now the velocity at the source.

When the jacobian is strictly positive, the solution in the time domain can be constructed straigtforwardly by

$$P(\mathbf{x}, t) = \frac{1}{2\pi}\int P(\mathbf{x}, \omega)\,e^{-i\omega t}\,d\omega \tag{6.78}$$

which gives

$$P(\mathbf{x}, t) = \frac{1}{4\pi}\sqrt{\frac{c(\mathbf{x})}{c_0 J(\mathbf{x})}}\,s(t - T(\mathbf{x}))\,. \tag{6.79}$$

Unfortunately, this simple expression is only valid at infinite frequency. For a finite frequency, any abrupt variation leads to different results. Moreover, a slight complication appears when the jacobian changes its sign or even when it vanishes. Situations giving this phenomenon are frequently met as shown for caustics in Figure 6.17. When the jacobian goes to zero, the ray tube section degenerates into a zero section: we are on a caustic and the ray theory is no longer valid because the amplitude of the signal will be infinite. Knowing the position of the caustic, it is possible to construct another asymptotic theory which takes into account the undulatory aspect of the signal and allows a description of interferences near the caustic or, equivalently a description of the propagation depending on the frequency. In fact, on the illuminated side of the caustic, many rays go through the same point giving the oscillating aspect of the amplitude (Figure 6.18), while on the other side of the caustic, we find an exponential decay depending on the frequency. What we must learn is the inversion of sign of J when we go through the caustic and that the Airy theory (Ludwig, 1966) permits us to connect the situa-

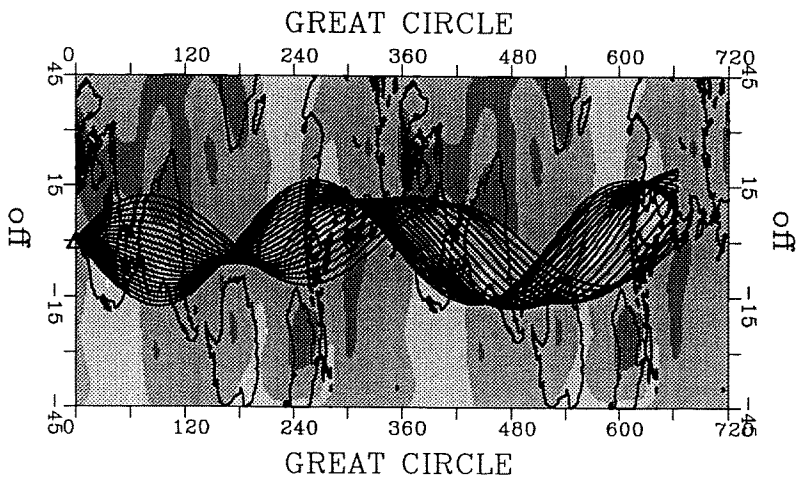

Figure 6.17 Caustics for surface-wave ray tracing on a heterogeneous sphere: focal points are blurred out. Heterogeneous model velocity is presented on gray scale on a rotated map of the Earth where the equator is the great circle between the source and the receiver.

tion on each side of the caustic. We find the initial form

$$\sqrt{\frac{c}{J}} \Rightarrow \sqrt{\frac{c}{|J|}} \cdot -i$$

$$\Rightarrow \sqrt{\frac{c}{|J|}} e^{-i\frac{\pi}{2}} \tag{6.80}$$

which introduces a phase shift when one goes through the caustic. The sign – is not given by the ray theory but by the Airy theory. This is the only contribution of the Airy theory considered here.

Formally we can write the phase shift in a suitable form

$$e^{-i\pi/2} = e^{-i\omega\frac{\pi}{2\omega}} \tag{6.81}$$

by exhibiting a frequency dependence of the travel-time: the wave arrives before expected. This phase shift induces the Hilbert transformation of the propagated signal which is written

$$P(\mathbf{x}, t) = \frac{1}{4\pi}\sqrt{\frac{c(\mathbf{x})}{c_0\,|J(\mathbf{x})|}}\,S(t - T(\mathbf{x})) \tag{6.82}$$

where S is the Hilbert transformation of S.

Let us recall that the Hilbert transformation $\mathcal{F}(t)$ of a function $F(t)$, defined as the principal value of the following integral,

$$\frac{1}{\pi}\int \frac{F(\tau)}{(t-\tau)}\,d\tau, \tag{6.83}$$

has a Fourier transformation $-i\,\mathrm{sgn}(\omega)\,F(\omega)$. We find that a function and its

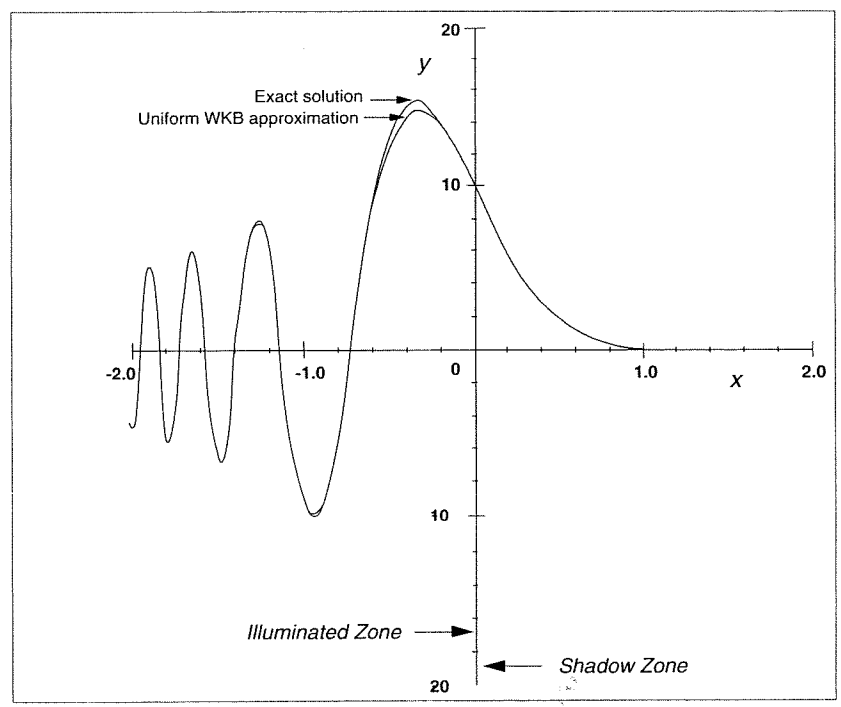

Figure 6.18 Amplitude oscillation and decrease from the two sides of the caustic. Please note the accuracy of the WKB or Ray theory very near the caustic.

Hilbert transform have the same spectrum, that the Hilbert transform acts in opposite phase to differentiation of the signal (Figure 6.19). The convolution formula can be deduced:

$$\frac{d}{dt}\frac{H(t)}{\sqrt{t}} * \frac{H(t)}{t-\tau} = \pi\delta(t-\tau). \tag{6.84}$$

Two Hilbert transformations must be noticed

$$\begin{aligned} \delta(t) &\rightarrow -\frac{1}{\pi t} \\ \frac{H(t)}{\sqrt{t}} &\rightarrow \frac{H(-t)}{\sqrt{-t}}, \end{aligned} \tag{6.85}$$

with a geometrical description given by Figure 6.20.

Of course, the sign inversion of the jacobian J might be repeated when the ray hits a new caustic. This phenomenon is often met in surface-wave ray tracing where, for geometrical reasons, waves are focused on the antipode of the source, then on the source again when the sphere is homogeneous. In order to keep track of these intersections with caustics, we introduce the KMAH index (for Keller, Maslov, Arnold and Hormander) initially taken as zero and which increases by 1 for each caustic. Moreover, when the ray tube section reduces to a single point in a three-dimensional medium, we count two crossings for the focal point (Chapman, 1985). We have the complete expression

$$P(\mathbf{x}, \omega) = S(\omega)\,\phi(\gamma_1, \gamma_2)\sqrt{\frac{c(\mathbf{x})}{|J(\mathbf{x})|}}\, e^{i\omega T(\mathbf{x})}\, e^{-i\frac{\pi}{2}\operatorname{sgn}(\omega)\,\mathrm{KMAH}}. \tag{6.86}$$

We can write the pressure in the time domain in the general form:

$$P(\mathbf{x}, t) = \mathcal{R}\{P(\mathbf{x})\,\bar{S}(t - T(\mathbf{x}))\} \tag{6.87}$$

where

$$P(\mathbf{x}) = \phi(\gamma_1, \gamma_2)\sqrt{\frac{c(\mathbf{x})}{|J(\mathbf{x})|}}\, e^{-i\frac{\pi}{2}\mathrm{KMAH}} \tag{6.88}$$

and $\bar{S}$ is the analytic function associated with the function S. Practically, we only consider positive frequencies which introduce a modification of Fourier transformation of real functions which are such that the value at the frequency $-\omega$ is equal to the complex conjugate of the value at the frequency ω. We can therefore

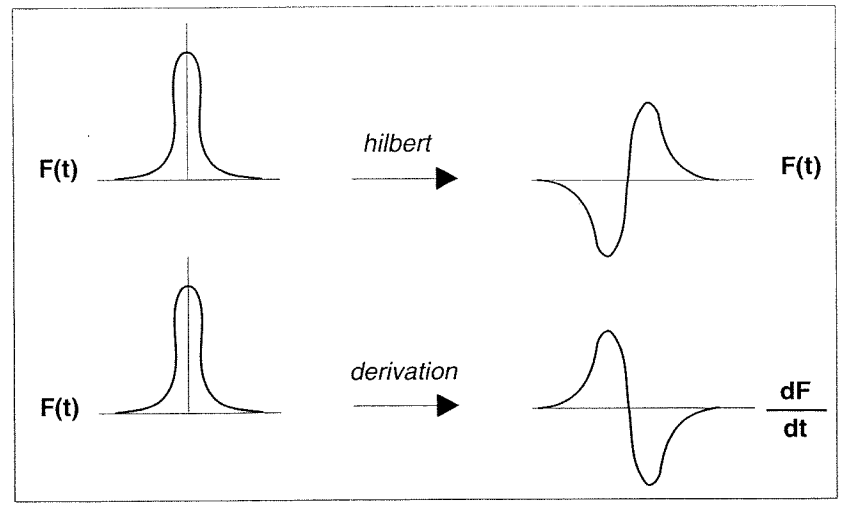

Figure 6.19 Comparison between Hilbert transform and differentiation.

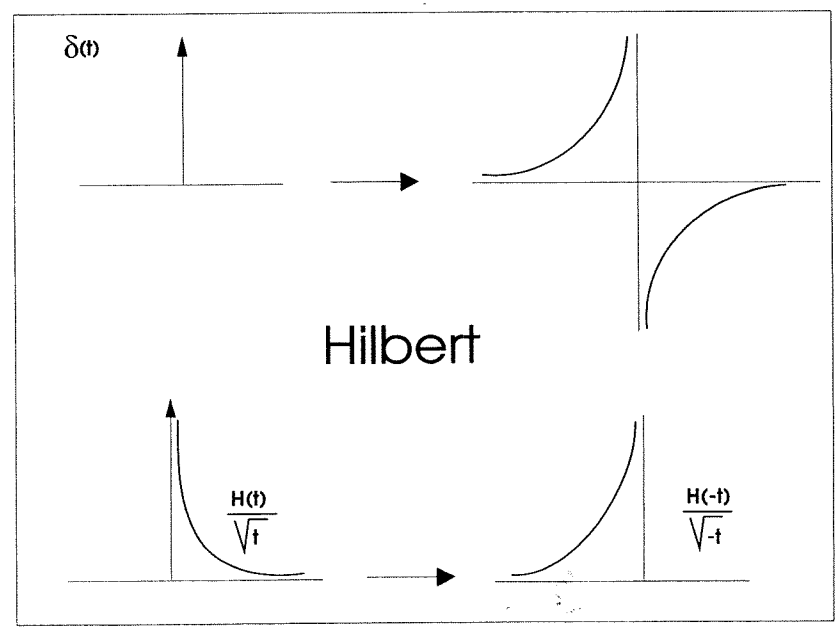

Figure 6.20 Geometrical description of two Hilbert transforms.

reduce the domain of integration and find

$$f(t) = \frac{1}{\pi} \mathcal{R} \int_0^\infty f(\omega)\, e^{-i\omega t}\, d\omega\,. \tag{6.89}$$

The following complex function

$$\tilde{f}(t) = \frac{1}{\pi} \int_0^\infty f(\omega)\, e^{-i\omega t}\, d\omega \tag{6.90}$$

has a Fourier transformation $2H(\omega)\, f(\omega)$. Its real part is $f(t)$. Its imaginary part F is written

$$F(t) = \frac{1}{\pi} \mathcal{R} \{ \int_0^\infty -if(\omega)\, e^{-i\omega t}\, d\omega \} \tag{6.91}$$

and reduces to

$$F(t) = \frac{1}{2\pi} \int_{-\infty}^\infty -i\,\mathrm{sgn}\,(\omega) f(\omega)\, e^{-i\omega t}\, d\omega \tag{6.92}$$

which shows that F is the Hilbert transformation of the function f. Therefore, the analytic function $\tilde{f}$ is the sum of the function and its Hilbert transformation. This is the justification of the use of the analytic function in the expression of the pressure when we consider only positive frequencies (Chapman, 1978).

For the zero-order approximation, we need now to estimate the ray trajectory, the travel-time T and the jacobian J at the point where we wish to evaluate the asymptotic solution. This task is technically difficult and we shall concentrate on it in two following sections. Before doing it, let us mention one additional point.

If we consider the next term of the series A_1, we have the following equation:

$$2\nabla T \cdot \nabla A_1 + \nabla^2 T A_1 = -\nabla^2 A_0 \tag{6.93}$$

or

$$\frac{\mathrm{div}\,(A_1^2 \nabla T)}{A_1} = -\nabla^2 A_0 \tag{6.94}$$

which shows that rapid variations of A_0 lead to significant amplitudes of the term A_1. This is the case near the critical angle for refracted waves, for converted phases S near the free surface and the construction of new solutions valid for these particular cases is a game enjoyed by many researchers.

6.5 Analytical examples of ray tracing

Let us first consider simple examples where tracing rays is rather straigthforward. We are looking for rays, travel-time and geometrical expansion coefficients from the differential system

$$\begin{aligned} \frac{d\mathbf{x}}{ds} &= c(\mathbf{x})\,\mathbf{p} \\ \frac{d\mathbf{p}}{ds} &= \nabla\left(\frac{1}{c(\mathbf{x})}\right). \end{aligned} \tag{6.95}$$

6.5.1 *Homogeneous media*

For a homogeneous medium $c(\mathbf{x}) = c_0$, the ray solution is simply straight segments. We find the following equations,

$$\begin{aligned} \mathbf{p}(s) &= \mathbf{p}_0 \\ \mathbf{x}(s) &= \mathbf{x}_0 + c_0\,(s - s_0)\,\mathbf{p}_0 \end{aligned} \tag{6.96}$$

where the position at s_0 is $\mathbf{x}_0$. The jacobian increases as r^2 in a three-dimensional medium and, consequently, the amplitude decreases as $1/r$. In a two-dimensional medium, the amplitude exhibits a typical tail from a variation in $1/\sqrt{r}$, while the one-dimensional propagation prevents any spreading and the amplitude is kept constant during the propagation.

6.5.2 *Constant gradient of the velocity*

Seismologists are often interested in a velocity structure which increases with depth (Ben-Mehahem and Singh, 1981). The simplest model one can think about is a linear increase with depth of the velocity: this does not mean that this leads to the simplest ray tracing. The following velocity structure

$$c(\mathbf{x}) = c_0 + \Gamma z \tag{6.97}$$

implies simple differential equations from eq. (6.95) for the components p_x and p_y of the slowness vector: they are constant along the ray. The ray is in a vertical plane without torsion and one can assume that p_y is set to zero by an appropriate selection of the coordinate system: the ray lies inside the plane $(x\,o\,z)$. The horizontal component p_x is called the ray parameter and denoted sometimes p. Let us introduce the angle θ between the vertical and the ray (Figure 6.21). This angle is a

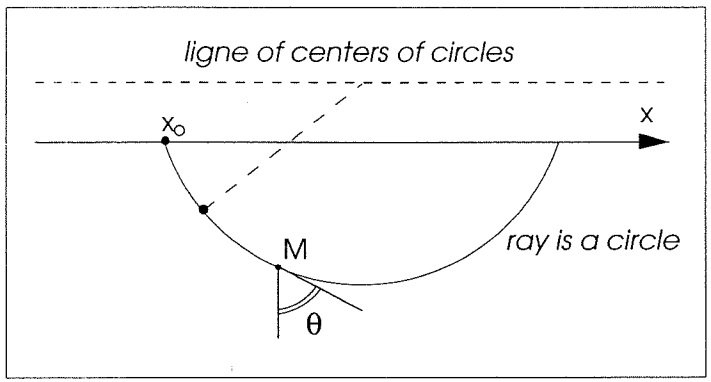

Figure 6.21 Geometry of rays in a medium with a constant gradient of velocity.

good parameter for tracking the ray itself. By definition of the tangent, we have

$$p_x(s) = \frac{\sin\theta(s)}{c(z)}$$
$$p_z(s) = \frac{\cos\theta(s)}{c(z)}. \tag{6.98}$$

The curvature $\mathcal{K}$ becomes constant through the equation

$$\mathcal{K} = \frac{1}{c(z)}\frac{dc}{dz}\sin\theta\Gamma p_x, \tag{6.99}$$

which means that the ray is a portion of a circle of radius $1/\Gamma p_x$. From the geometrical definition of the curvature (Figure 6.13), one can deduce the evolution of the angle θ by

$$\frac{d\theta}{ds} = \mathcal{K} = \Gamma p_x. \tag{6.100}$$

With this parameter, one can integrate the ray tracing equations

$$x - x_0 = \int_{x_0}^{x} dx' = \int_{\theta_0}^{\theta}\frac{dx}{ds}\frac{ds}{d\theta'}d\theta' = \frac{1}{\Gamma p_x}\int_{\theta_0}^{\theta}\sin\theta'\,d\theta'$$
$$z - z_0 = \int_{z_0}^{z} dz' = \int_{\theta_0}^{\theta}\frac{dz}{ds}\frac{ds}{d\theta'}d\theta' = \frac{1}{\Gamma p_x}\int_{\theta_0}^{\theta}\cos\theta'\,d\theta' \tag{6.101}$$

and obtain analytical trajectories starting from θ_0

$$x - x_0 = \frac{1}{\Gamma p_x}(\cos\theta_0 - \cos\theta)$$
$$z - z_0 = \frac{1}{\Gamma p_x}(\sin\theta - \sin\theta_0). \tag{6.102}$$

With the help of the trigonometric expression $\sin^2\theta + \cos^2\theta = 1$, we find the equation of a circle

$$(x - x_0 - (1/\Gamma p_x)\cos\theta_0)^2 + (z - z_0 + (1/\Gamma p_x)\sin\theta_0)^2 = (1/\Gamma p_x)^2. \tag{6.103}$$

If we assume x_0, z_0 (related to θ_0) as the system origin, one can find the simplified equation

$$(x - (1/\Gamma p_x)\cos\theta_0)^2 + (z + c_0/\Gamma)^2 = (1/\Gamma p_x)^2 \tag{6.104}$$

which shows that the circle centers of rays for different shooting angles belongs to a straigth line $z + c_0/\Gamma = 0$ (Figure 6.21). The travel-time T is deduced by direct integration

$$T - T_0 = \int_{s_0}^{s} u\,ds' = \int_{\theta_0}^{\theta}\frac{1}{c}\frac{ds}{d\theta'}d\theta' = \frac{1}{\Gamma}\int_{\theta_0}^{\theta}\frac{1}{\sin\theta'}\,d\theta' \tag{6.105}$$

which gives the final analytical expression

$$T = T_0 + \frac{1}{\Gamma}\mathrm{Log}\left[\frac{\tan(\theta/2)}{\tan(\theta_0/2)}\right]. \tag{6.106}$$

For the geometrical spreading evaluation, one must express the coordinate x with respect to the initial angle at constant depth z through

$$\cos\theta = \sqrt{1 - \frac{c^2}{c_0^2}\sin^2\theta_0} \tag{6.107}$$

which gives

$$x - x_0 = \frac{1}{\Gamma p x}\left(\cos\theta_0 - \sqrt{1 - \frac{c^2}{c_0^2}\sin^2\theta_0}\right). \tag{6.108}$$

The estimation of the jacobian

$$J(\theta) = \left|\frac{\partial x}{\partial\theta_0}\right|_z\cos\theta \tag{6.109}$$

allows the analytical computation of the amplitude for this simple velocity distribution.

6.5.3 *Constant gradient of the square of the slowness*

Another example which gives the simplest solution for ray tracing is a constant gradient of the square of slowness u. The square of the slowness, related to the square of the refraction index widely used in scattering theory, has been disregarded by seismologists because this parametrization leads to a decrease of the velocity rather an increase with the depth. Therefore, an increase with depth can be obtained through a decomposition in finite layers where the gradient of the square of slowness is constant in each layer. The simplicity of the solution in each cell might overcome the penalty of a denser discretization with this choice of the velocity representation (Červený, 1987; Virieux *et al.*, 1988) (Figure 6.22).

The velocity structure is defined by the square of the slowness

$$u^2 = u_0^2 + \gamma \cdot \mathbf{x} \tag{6.110}$$

with a vectorial representation. The use of vectorial notation shows the separability property of the square of slowness between what happens along the x axis and along the z axis. This advantage avoids any rotation in order to align the gradient towards only one direction, rotation being required for the previous example of the constant gradient of the velocity. Associated with this distribution, a new parametrization τ of the ray defined as $ds = ud\tau$ allows the simplification of the

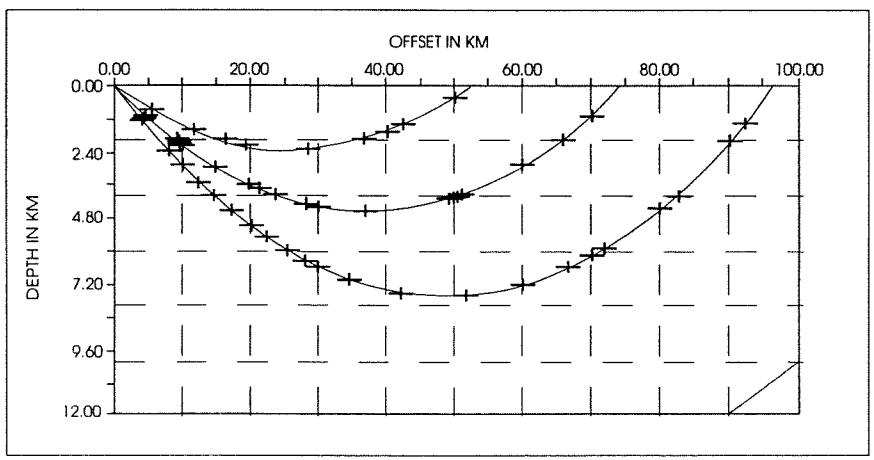

Figure 6.22 Rays for a linear increase of velocity assuming a local discretization of the velocity such that the square of slowness has a constant gradient: rays as circles agree perfectly. This is an illustration of the finite element approach where the number of points along one ray is rather small.

differential system (6.95) to

$$\frac{d\mathbf{x}}{d\tau} = \mathbf{p}$$

$$\frac{d\mathbf{p}}{d\tau} = \frac{1}{c(\mathbf{x})}\nabla_x\left(\frac{1}{c(\mathbf{x})}\right) = \frac{1}{2}\nabla_x u^2(\mathbf{x}) = \gamma/2. \tag{6.111}$$

The analytical ray is a parabola given by

$$\mathbf{x} = \mathbf{x}_0 + \mathbf{p}_0(\tau - \tau_0) + \frac{1}{4}\gamma(\tau^2 - \tau_0^2) \tag{6.112}$$

$$\mathbf{p} = \mathbf{p}_0 + \frac{1}{2}\gamma(\tau - \tau_0), \tag{6.113}$$

while the travel-time T is obtained by direct integration

$$T = T_0 + \int_{\tau_0}^{\tau} u^2 d\tau' = T_0 + \int_{\tau_0}^{\tau} (u_0^2 + \gamma \cdot \mathbf{x})\, d\tau'$$

$$T = T_0 + (u_0^2 + \gamma \cdot (\mathbf{x}_0 - \mathbf{p}_0\tau_0 - 1/4\gamma\tau_0^2))(\tau - \tau_0)$$

$$+\frac{1}{2}\gamma \cdot \mathbf{p}_0(\tau^2 - \tau_0^2) + \frac{1}{12}\gamma^2(\tau^3 - \tau_0^3). \tag{6.114}$$

The jacobian is estimated at constant τ by

$$J = \mathbf{n} \cdot \frac{\partial \mathbf{x}}{\partial \theta_0} \tag{6.115}$$

which becomes an expression increasing with τ

$$J = (\tau - \tau_0)\, p_0 = (\tau - \tau_0)\, u_0. \tag{6.116}$$

Many other velocity distributions lead to analytical expressions and our purpose is not to investigate all of them. Let us just underline that the distribution of the velocity in $\cosh(z)$ relates ray tracing on a homogeneous sphere to ray tracing in a two-dimensional medium for this particular distribution. Even more, using a transformation based on the hyperbolic cosine, the body-wave ray tracing programs can be adapted for surface-wave ray tracing. This distribution has also been studied intensively in fiber optics as an approximation to quadratic evolution of the refraction index away from the center of the optical fiber, the hyperbolic cosine giving analytical solutions (Mikaelian, 1980).

6.6 Arbitrary variation along one direction

6.6.1 *Ray tracing as quadrature equations*

Arbitrary variation along one direction is a natural extension from previous simple examples and has concentrated the attention of seismologists (see, for example, the textbook of Bullen, 1959) because the variation of the velocity structure inside the Earth is mainly along the depth direction (Figures 6.3 and 6.23). The slowness component $p_\perp$ perpendicular to this direction taken as z is constant because the velocity does not vary along this perpendicular direction:

$$\frac{dp_\perp}{ds} = \nabla_\perp \left(\frac{1}{c}\right) = 0 . \tag{6.117}$$

The ray lies inside a vertical plane that one can define as the plane (xoz). This argument follows the same line as the one presented for a constant gradient of the velocity and shows its generality. The differential system (6.95) reduces to the following system

$$\begin{aligned} \frac{dx}{ds} &= c(z)\,p_x \\ \frac{dz}{ds} &= c(z)\,p_z \end{aligned} \tag{6.118}$$

$$\begin{aligned} \frac{dp_x}{ds} &= 0 \\ \frac{dp_z}{ds} &= \frac{d}{dz}\frac{1}{c(z)} . \end{aligned} \tag{6.119}$$

Instead of using the curvilinear abscissa s as the parameter along the ray, one can use the coordinate z which controls the velocity variation. Because p_x is constant, the eikonal equation allows deduction of p_z from p_x. The evolution of x and p_x determines perfectly the ray and one has to solve a one-dimensional problem: this is the Landau reduction widely applied in physics. Because p_x is constant, we go down to a single equation

$$\frac{dx}{dz} = \frac{p_x}{p_z} = \frac{p_x}{\pm\sqrt{u^2(z) - p_x^2}} \tag{6.120}$$

with the implicit equation $dp_x/dz = 0$ as associated equation (Madariaga, 1984). The unknown sign is deduced from initial conditions. We obtain for a ray point-

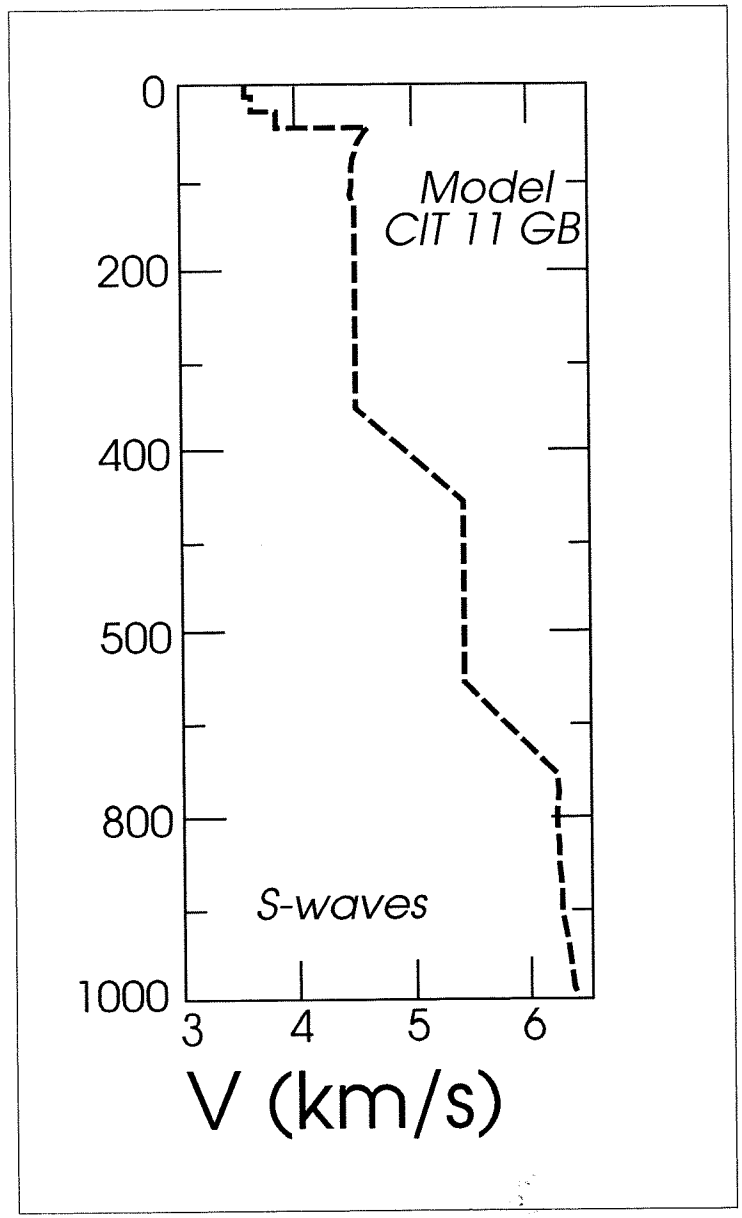

Figure 6.23 A depth dependent velocity structure inside the Earth for S waves.

ing initially downwards ($z > 0$) the following expression of the position X:

$$X(z, p_x) = X_0 + \int_{z_0}^{z} \frac{p_x}{\sqrt{u^2(z) - p_x^2}}\, dz. \tag{6.121}$$

At the depth z_p where the slowness parameter taken as the horizontal component of the slowness vector verifies $p_z^2 = u^2(z_p)$, the ray has a turning point and the integral (6.121) has an integrable singularity as long as du^2/dz does not vanish at this particular point. We end up with the final expression

$$X(z, p_x) = X_0 + \int_{z_0}^{z_p} \frac{p_x}{\sqrt{u^2(z) - p_x^2}}\, dz + \int_{z}^{z_p} \frac{p_x}{\sqrt{u^2(z) - p_x^2}}\, dz. \tag{6.122}$$

From the travel-time expression $dT = uds$, one deduces

$$\frac{dT}{dz} = \frac{1}{c^2(z)\, p_z} = \frac{u^2(z)}{\pm\sqrt{u^2(z) - p_x^2}} \tag{6.123}$$

and the known expression

$$T(z, p_x) = T_0 + \int_{z_0}^{z_p} \frac{u^2(z)}{\sqrt{u^2(z) - p_x^2}}\, dz + \int_{z}^{z_p} \frac{u^2(z)}{\sqrt{u^2(z) - p_x^2}}\, dz. \tag{6.124}$$

This expression is the basic formula for recovering the vertical velocity structure from travel-time data and has been used in many inverse problem formulations (Aki and Richards, 1980).

Combining expressions of the offset X and the travel-time allows cancelation of the singularity under the integral expression. The linear expression

$$\mathcal{T} = T - p_x X = T_0 - p_x x_0 + \int_{z_0}^{z} \sqrt{u^2(z) - p_x^2}\, dz \tag{6.125}$$

is often called the intersection time from the graphical interpretation given by Figure 6.24. This quantity taken as a function of p_x is a monotonic decreased function which was not the case for the offset X because

$$\frac{d\mathcal{T}}{dp_x} = \frac{dT}{dp_x} - X - p_x \frac{dX}{dp_x} = -X. \tag{6.126}$$

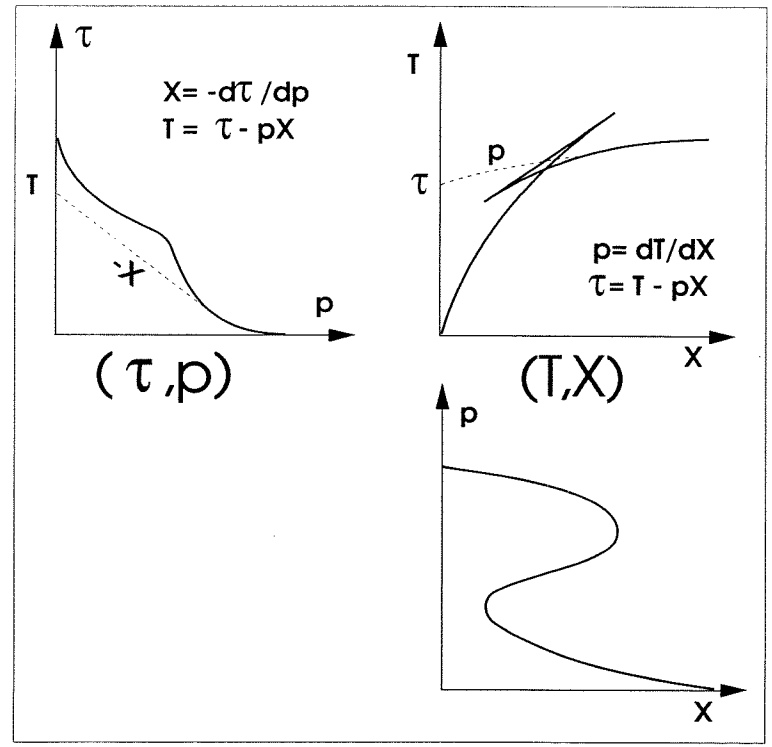

Figure 6.24 Unfolding the triplication by using the function τ instead of travel-time T. The intersection time τ is a monotonic function of $p_x = p$. The function p of the variable x allows the estimation of the amplitude.

This intersection time appears naturally in analytical inverse formulations of the travel-time (Stoffa, 1989) and the new function

$$\mathcal{I}(X_0, p_x) = \mathcal{T}(p_x) + X_0 p_x \tag{6.127}$$

has a derivative equal to zero for the point X_0. Geometrical rays arriving at point X_0 are the extrema of the function $\mathcal{I}(X_0, p_x)$ (Figure 6.25). Once the different parameters p are known, the geometrical spreading of each ray comes from the derivative of the function $x(p_x)$ (Figure 6.25). We shall see that synthetic seismograms require either contributions of these geometrical rays for the ray theory or contributions of adjacent rays for the WKBJ theory which cannot reach the station. More complex theories as the Cagniard and De Hoop approach (Helmberger, 1996, this issue) are based on an extension in a complex p plane of this function $\mathcal{I}$.

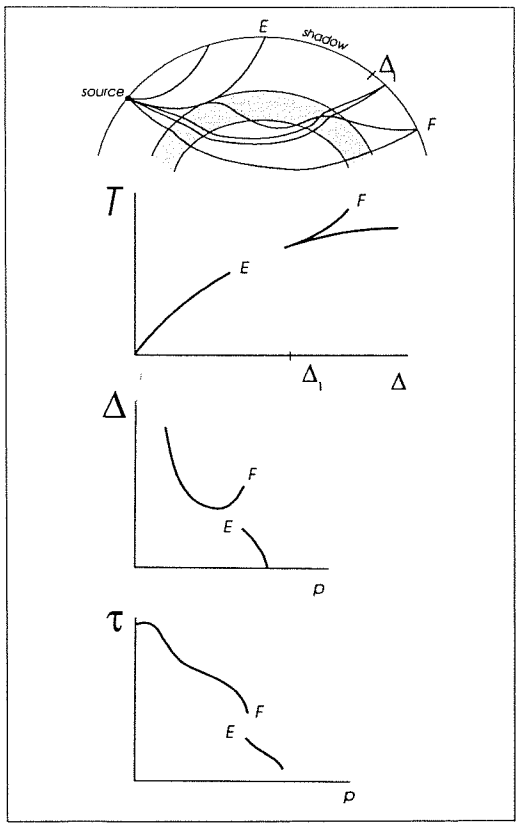

Figure 6.25 Interpretation of travel-time T, station position Δ and intersection time τ for a shadow zone.

When the source and the station are at the free surface of the Earth, we find basic formula from eqs. (6.121) and (6.124) for radial distance $R(p)$ and travel-time $T(p)$

$$R(p) = 2\int_0^{z_p} \frac{p}{\sqrt{u^2(z) - p^2}}\, dz \tag{6.128}$$

$$T(p) = 2\int_0^{z_p} \frac{u^2(z)}{\sqrt{u^2(z) - p^2}}\, dz \tag{6.129}$$

which have a great importance for the Earth structure (Aki and Richards, 1980). The extension in spherical coordinates does not change basic results (Chapman and Orcutt, 1985).

6.6.2 *Triplication and shadow zones*

The triplication zone associated with a sharp increase of the velocity as, for example, the first-order discontinuity of 670 km, will give an inflexion of the $\mathcal{T}$ curve as shown on previous Figure 6.24. Multiple arriving signals are observed at a given station. On the other hand, a shadow zone associated with a low-velocity zone will result in a jump of the τ parameter and no signal would be observed if we follow the ray theory (Figure 6.25).

Let us resume the procedure to construct quantities required to estimate seismograms. From an observed travel-time curve R, T (Figure 6.26a), one can find the slope which is nothing more than the parameter p (Figure 6.26b) or the derivative of the slope (Figure 6.26c). The integration of the eq. (6.126) will construct the function $\mathcal{T}$ as a function of p (Figure 6.26d).

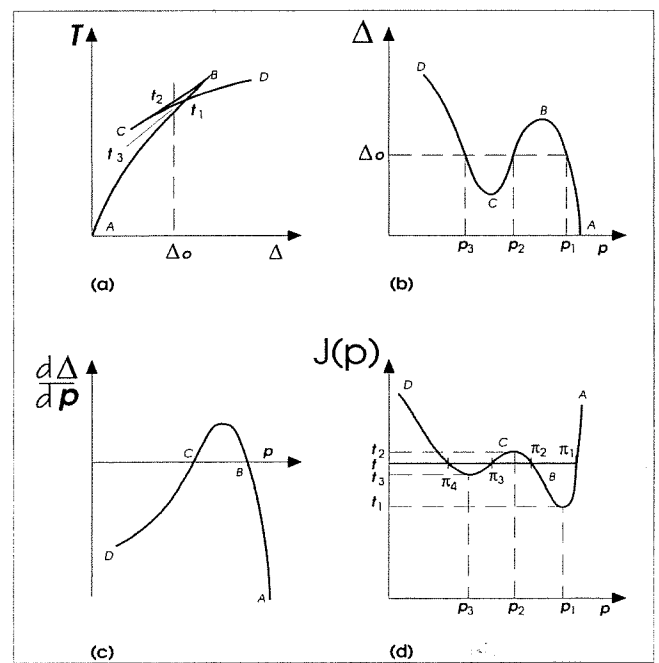

Figure 6.26a-d Analysis of a triplication with the function $\mathfrak{I}(x_0, p_0)$. The p variables associated with a ray arriving at station Δ_0 are extrema of this function.

6.7 Variational approach

Another way to define the ray is based on variational arguments. The ray between a source and a receiver is the trajectory with the minimum travel-time. In fact, one can state more precisely the Fermat principle for which the ray is the trajectory of travel-time extrema. This approach is very interesting because it seems more adapted to the seismological problem where the ray must connect the source and the receiver while the problem solved previously is a problem with initial conditions: the ray leaves the source with a preselected direction.

6.7.1 *Euler equations*

Variational calculus demonstrates that, if the function f is such that the following integral

$$\int_1^2 f(v, \mathbf{x}, \dot{\mathbf{x}})\, dv \tag{6.130}$$

is extremum, the function verifies the local differential equation, called Euler equation,

$$\nabla_x f - \frac{d}{dv}\nabla_{\dot{x}} f = 0\,. \tag{6.131}$$

Let us apply this variational principle to the travel-time T which is an extremal function as stated by Fermat principle and which is defined as an integral between points $\mathbf{x}_1$ and $\mathbf{x}_2$

$$T(\mathbf{x}_1, \mathbf{x}_2) = \int_1^2 u(\mathbf{x})\, ds = \int_1^2 u[\mathbf{x}(\xi)] \parallel \dot{\mathbf{x}} \parallel d\xi \tag{6.132}$$

where ξ is an independent parameter defined by $\parallel \dot{\mathbf{x}} \parallel d\xi = ds$. The curvilinear abscissa s is not an independent parameter because it is related to the total length L of the ray by

$$\int_1^2 ds = L\,. \tag{6.133}$$

The local differential equation comes from expression (6.131)

$$\parallel \dot{\mathbf{x}} \parallel \nabla_x u = \frac{d}{d\xi}\left[(u(\mathbf{x}))\, \frac{\dot{\mathbf{x}}(\xi)}{\parallel \dot{\mathbf{x}}(\xi) \parallel}\right] \tag{6.134}$$

and might be converted into the curvature equation

$$\nabla_x u = \frac{d}{ds}\left(u\, \frac{dx}{ds}\right) \tag{6.135}$$

by eliminating the variable ξ. The equivalence between ray tracing equations (local equations) and Fermat principle (global approach) is demonstrated.

6.7.2 *Lagrangian formulation*

One can exploit the lagrangian formalism in more detail. The function f is often called Lagrangian $\mathcal{L}$ and is given by

$$\mathcal{L} = u[x(\xi)] \parallel \dot{\mathbf{x}} \parallel \tag{6.136}$$

for the specified sampling parameter ξ. Other definitions are possible and might be more adapted to ray theory than the previous straigtforward definition. The lagrangian, whatever it is, is often split in two terms which separate the dependence in $\mathbf{x}$ and $\dot{\mathbf{x}}$ with the formula

$$\mathcal{L} = E_c(v, \dot{\mathbf{x}}) - E_p(v, \mathbf{x}) \tag{6.137}$$

and the local equation becomes

$$-\frac{d}{dv}\nabla_{\dot{x}} E_c = \nabla_x E_p\,. \tag{6.138}$$

In order to apply this separation to eq. (6.134), we need to avoid the term $\parallel \dot{\mathbf{x}} \parallel$ on the left hand side and the term depending in $\mathbf{x}$ on the right end side. The simplest way is to absorb $u(\mathbf{x})$ in our choice of the sampling parameter which becomes $ds = ud\tau$ and gives the simple equation

$$-\frac{d\dot{\mathbf{x}}}{d\tau} = -u(\mathbf{x})\nabla_x u(\mathbf{x}) \tag{6.139}$$

where $\dot{\mathbf{x}}$ stands now for $d\mathbf{x}/d\tau$. The expressions for E_c and E_p are the following

$$E_c = \frac{1}{2} \parallel \dot{\mathbf{x}} \parallel^2$$

$$E_p = -\frac{1}{2} u^2(\mathbf{x}). \tag{6.140}$$

Of course, the choice of these functions is not unique and we are guided by the mechanical analogy of kinetic energy for E_c and potential energy E_p.

The travel-time can be written with the Lagrangian $\mathcal{L}$ as

$$T(\mathbf{x}_1, \mathbf{x}_2) = \int_1^2 \mathcal{L}(\mathbf{x}(\xi))\, d\xi. \tag{6.141}$$

6.7.3 *Hamiltonian formulation*

We introduce the quantity $\mathbf{p} = \dot{\mathbf{x}}$ as an independent variable and we switch from the lagrangian formalism towards the hamiltonian formalism with this new variable. The Hamiltonian $\mathcal{H}$ is deduced from the Lagrangian $\mathcal{L}$ (Landau and Lifchitz, 1969) by

$$\mathcal{H} = p\,\dot{\mathbf{x}} - \mathcal{L}(\mathbf{x}, \mathbf{p}) = \frac{1}{2}\left[p^2 - u^2(\mathbf{x})\right]. \tag{6.142}$$

To this Hamiltonian are associated differential equations on which we concentrate our attention in the next section. Let us just write down the expression of the travel-time with the help of the hamiltonian

$$T(\mathbf{x}_1, \mathbf{x}_2) = \int_1^2 [\mathbf{p}\cdot\dot{\mathbf{x}} - H(\mathbf{x}, \mathbf{p})]\, d\tau. \tag{6.143}$$

Of course, selecting classical ray tracing, Lagrangian ray tracing or Hamiltonian ray tracing is a matter of personal convenience either because one approach is much easier than other ones or because numerical stability comes with one specific approach. Whatever is our choice, we should end up as in mechanics with the same solution for the ray. We shall see that this feature is quite different for perturbation techniques which provide coordinate-dependent results. Recent discussions in the geophysical literature have raised the problem of equivalence of these approaches (Snieder and Sambridge, 1992, 1993; Moore, 1994a,b; Farra *et al.*, 1994).

6.8 Validity of the ray theory

Before going into more detail in the ray tracing equations for arbitrary heterogeneous medium, let us go back to the high frequency approximation and discuss the domain of validity of this theory and when one expects it to break-down (Červený, 1985).

6.8.1 *Validity of the asymptotic approach*

The definition of the ray as the mathematical solution of the eikonal equation gives an object without any thickness while rays observed in physics have certainly a given thickness associated with the frequency content of the propagated wavefield (Kravtsov and Orlov, 1990, p. 87). The high frequency approximation means that the wavelength λ of the propagating signal is lower than any spatial scales L associated with heterogeneities. One can think about velocity variations or interface curvatures. Often the wavelength is comparable with the spatial scale. When irregularities exist, the high frequency solution must feel variation over a wavelength in order to avoid any interferences. That is the first heuristic criterion one must verify saying that gradients of phase and amplitude must not vary significantly around the ray. This volume, where these variations are insignificant, will be called the Fresnel volume. Moreover, the total distance D travelled by wavefronts should be significantly lower than L^2/λ, because over that distance D rays will interfere. This condition prevents the ray theory to be applicable beyond a given distance which is not often found in seismology: for example, ray theory could not be applied to the interpretation of the surface-wave train R4 because the distance is too large. If we consider the ray as a physical object, the Fresnel volume should be considered as the region where the ray is localized.

When these conditions are fulfilled, the source wavelet propagates without distortion and only the amplitude is modulated. Unfortunately, irregularities are found and the ray theory fails. These failures can be classified in order to detect them and, when possible, to overcome them (Chapman, 1985; Hanyga, 1989).

6.8.2 *Classification*

It is useful to describe standard situations we possibly meet during ray tracing: they are canonical ray problems already described in many papers.

1) *Normal and turning rays* – This is the simplest case where the medium contains no discontinuities and the ray paths as well as smoothly varying amplitudes (Figure 6.27). Ray theory in this case works fine.

2) *Reversed rays* – If rays cross, then the amplitude becomes infinite and ray theory breaks down (Figure 6.28). Special methods are needed in the vicinity of this singularity, called caustic. Nethertheless, ray theory can be used before and after the caustic provided we take care of the amplitude correctly as already described.

3) *Reflected and transmitted rays* – When an interface has a smooth variation and the reflection/transmission coefficient varies gently, ray theory works for reflected/transmitted rays. Amplitudes are modified by reflection/transmission coefficients and by the interface curvature (Figure 6.29). Total reflections are possible with complex coefficients.

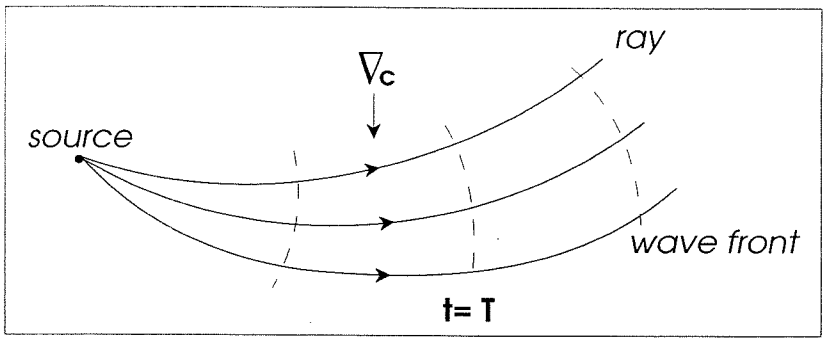

Figure 6.27 Normal turning rays with wavefronts shown in dashed line after Chapman (1985).

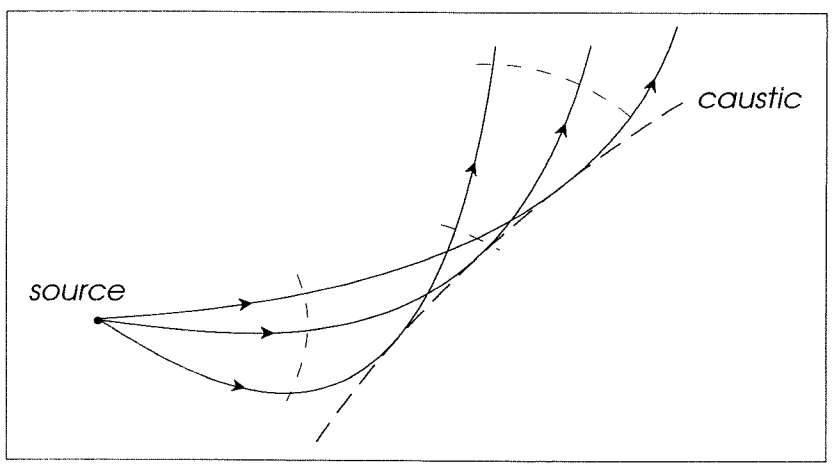

Figure 6.28 Reversed rays after touching a caustic after Chapman (1985).

These previously mentioned rays can be described by ray theory while the following rays are not handled by the ray theory in its simple form.

4) *Critical rays and head waves* – At the critical angle, the reflection coefficient has a square root singularity and the grazing transmitted ray has a zero geometrical amplitude. The discontinuity in the reflected wavefront and the transmitted wavefront are connected by another wavefront, the head wave (Figure 6.30). Simple ray theory does not describe the critical region and the head wave. More elaborate high frequency theories are required.

5) *Interference head waves* – A simple head wave rarely exists. Invariably, a velocity gradient or the curvature of the interface cause a turning ray with similar travel-time and create interferences (Figure 6.31). Taking care of this interference will require careful counting of rays by the theory. More appropriate approximations are required for the lower medium or for the interface interaction.

6) *Airy caustics* – In the vicinity of the caustic, there is interference between normal rays and reversed rays (Figure 6.28). Taking care of this interference re-

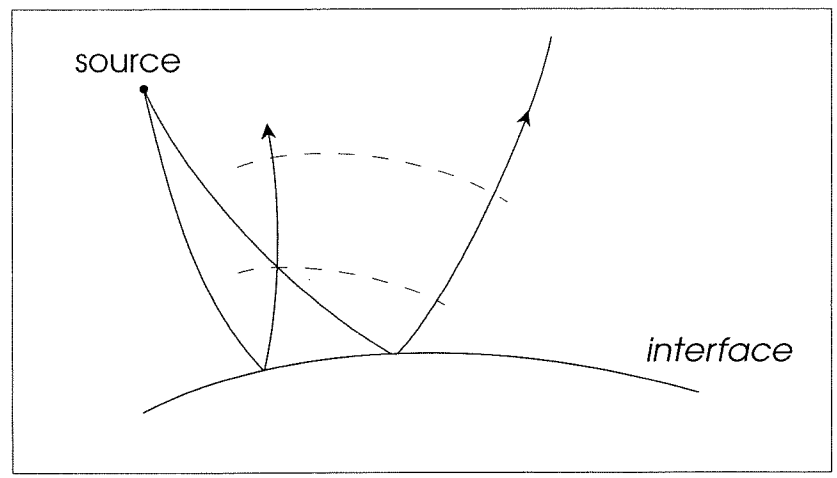

Figure 6.29 Rays reflected from a curved interface after Chapman (1985).

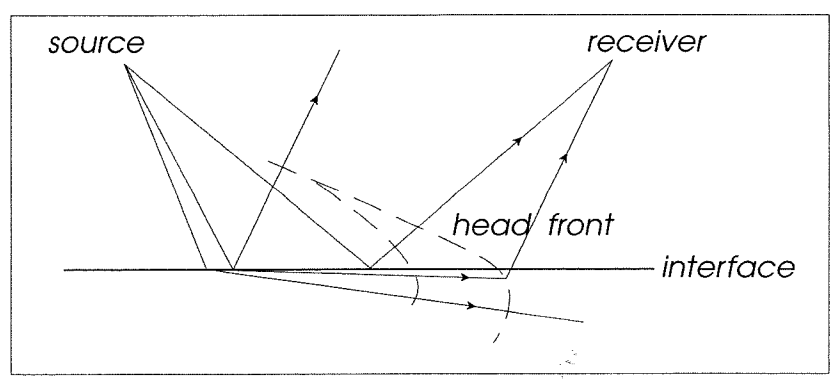

Figure 6.30 A critical reflection and transmission, total reflection and head wave after Chapman (1985).

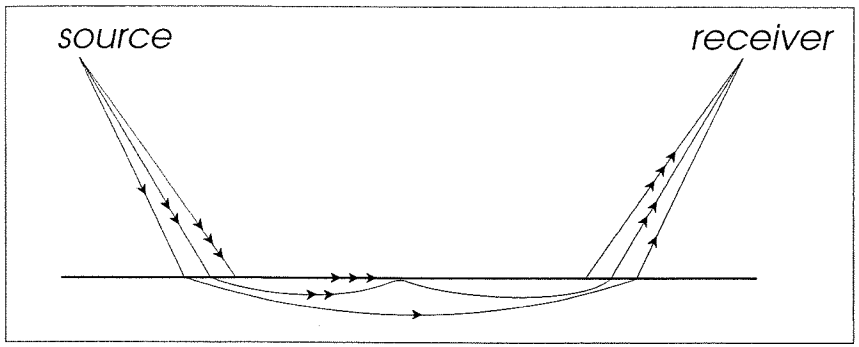

Figure 6.31 Rays contributing to an interference head wave. Only one multiple refraction is shown and no attempt is made to include wavefronts after Chapman (1985).

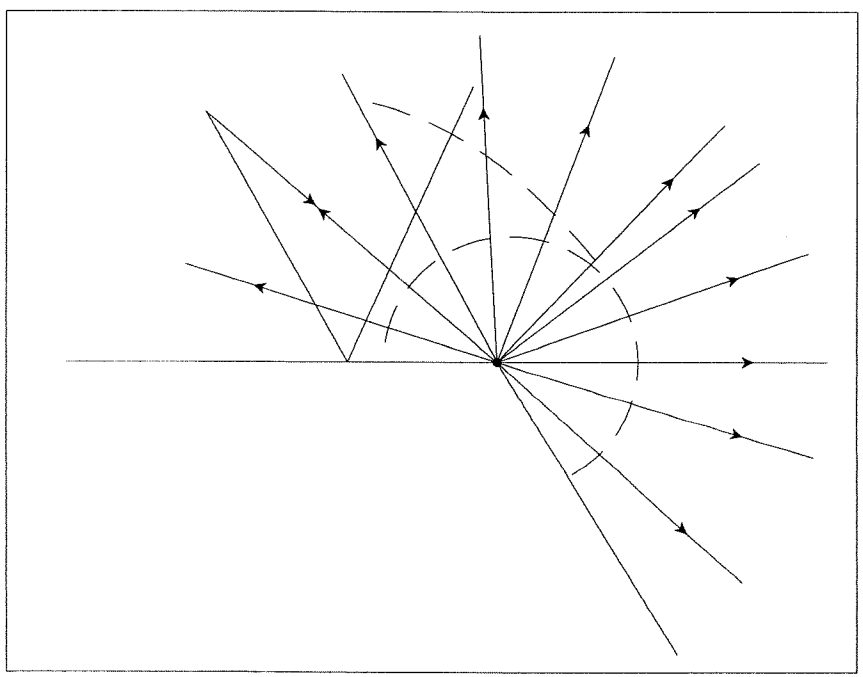

Figure 6.32 Reflection and diffraction from a corner after Chapman (1985).

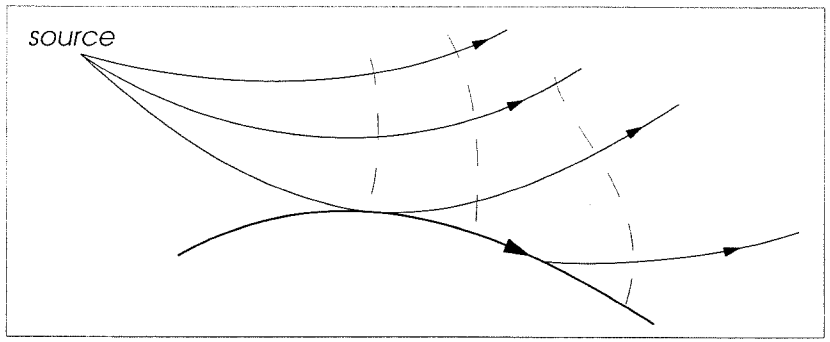

Figure 6.33 Rays grazing an interface and diffracting along it after Chapman (1985).

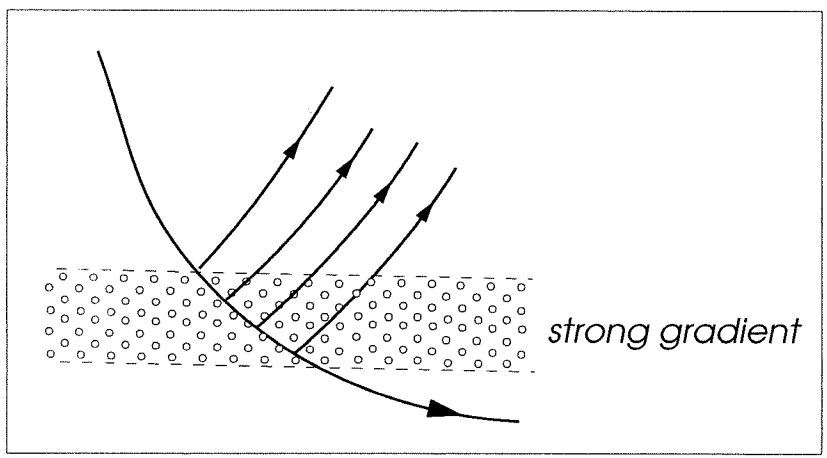

Figure 6.34 A ray is propagation through a region of high gradient and being reflected continuously after Chapman (1985).

quires a more elaborate ansatz than the Airy function in the frequency domain.

7) *Edge and point diffractions* – If an interface is discontinuous, diffracted signals are generated at the corner (Figure 6.32). Geometrical diffraction theory can be used to model diffraction by the corner with frequency-dependent diffraction coefficient obtained by a local canonical problem.

8) *Interface diffractions* – If a ray grazes an interface (Figure 6.33), a discontinuity in the wavefront is generated and an interface wave described the decay in the created shadow. It is necessary to solve boundary conditions for a grazing ray and an interface. The amplitude and the travel-time of the signal are frequency-dependent.

9) *Gradient coupling* – When a strong gradient of velocity is present, reflected and transmitted waves are observed when the wavelength of the source signal is noticeable compared with the thickness of the area with strong gradient (Figure 6.34). Iterative methods handle this problem as proposed by Chapman and coworkers (Chapman and Coates, 1994).

6.9 Ray tracing in heterogeneous media

Tracing rays requires solving a non-linear ordinary differential equation or a system of non-linear ordinary differential equations depending on the number of variables we consider. This problem is a rather simple one if we assume initial conditions, *i.e.* initial position and initial slowness vector. The problem with boundary conditions where the ray must connect two points is more difficult. Unfortunately, the second is the one we face in geophysics because we need rays arriving at stations.

6.9.1 *Setting up ray tracing equations*

Many formulations exist for the initial value problem: I select an approach based on the hamiltonian formulation (Farra and Madariaga, 1987; Virieux *et al.*, 1988; Farra *et al.*, 1989). The hamiltonian approach is not strictly necessary in this lecture but its relative simplicity and its elegance justify in itself this introduction. The power of this formulation is still a research investigation (Abdullaev, 1993).

The general hamiltonian we consider is related to the eikonal equation and is an extension to the one found in eq. (6.142). We consider the hamiltonian

$$H(\xi, \mathbf{x}, \mathbf{p}) = f(\mathbf{x})\,[p^2 - u^2(\mathbf{x})] \tag{6.144}$$

which is equal to zero from the eikonal eq. (6.41). The choice of the variable ξ, which is a sampling parameter, is related to the choice of the hamiltonian and, for example, the particular hamiltonian

$$H(\tau, \mathbf{x}, \mathbf{p}) = \frac{1}{2}[p^2 - u^2(\mathbf{x})] \tag{6.145}$$

is related to the parameter τ defined by $ds = u(\mathbf{x})\,d\tau$ (Burridge, 1976). Whatever is the selected hamiltonian, characteristic equations are associated and have the universal form:

$$d\xi = \frac{dx_i}{\nabla_{p_i} H} = \frac{dp_i}{-\nabla_{p_i} H}\,. \tag{6.146}$$

We call these equations canonical equations for their generality. The ray is defined by its canonical vector,

$$y(\xi) = \begin{pmatrix} \mathbf{x}(\xi) \\ \mathbf{p}(\xi) \end{pmatrix} \tag{6.147}$$

which satisfies the following equations for the particular hamiltonian we have selected

$$\begin{aligned} \frac{d\mathbf{x}}{d\tau} &= \nabla_{\mathbf{p}} H = \mathbf{p} \\ \frac{d\mathbf{p}}{d\tau} &= -\nabla_{\mathbf{x}} H = \frac{1}{2}\nabla_{\mathbf{x}} u^2(\mathbf{x}). \end{aligned} \tag{6.148}$$

The first equation is the definition of the slowness vector if one remembers the relation between τ and s. The second is the curvature equation. The sampling parameter τ defines the structure of the hamiltonian which turns out to be a very simple one. Other choices of sampling parameters and associated hamiltonians are possible and lead to other differential equations but to the same trajectories, which are rays: we have the freedom to select the most suitable hamiltonian for the problem at hand.

We have extented the space of variables to what is called phase space with 6 variables in a three-dimensional medium. Because the slowness vector is a very important quantity for rays, this extension is of practical interest for us. For the Lagrangian formulation, this extension is not performed, giving an apparent benefit to this approach cancelled by the more complex structure of the ray equations.

The travel-time is connected to the hamiltonian by a subtle relation which is not describe here. Let us mention only the relation needed to compute it in the general case

$$d\xi = \frac{dT}{\mathbf{p} \cdot \nabla_{\mathbf{p}} H} \tag{6.149}$$

which becomes for our particular hamiltonian

$$d\tau = \frac{dT}{p^2} = \frac{dT}{u^2}\,, \tag{6.150}$$

an already mentioned equation.

The number of free parameters in the three-dimensional space is not the number of variables of the phase space, *i.e.* 6 variables. The eikonal equation re-

duces to five this number while the implicit parameter ξ reduces to four the number of degrees of freedom. One can think about inverting both eqs. of (6.147) and equating the variable ξ of these inverted equations which gives this extra condition for going down to four independent variables.

This reduction of variables could be exploited in the phase space itself in order to solve differential equations for the minimum of variables. Following this idea, one can deduce a reduced hamiltonian from the previous one which was constant with the help of the eikonal equation. A simple way is to select one cartesian variable as the sampling parameter and to write the new hamiltonian from the eikonal equation

$$H(z, x, y, p_x, p_y) = -p_z = -\sqrt{u^2(x, y, z) - p_x^2 - p_y^2} \tag{6.151}$$

with equations

$$\begin{aligned}
\frac{dx}{dz} &= \frac{\partial H}{\partial p_x} = \frac{p_x}{\sqrt{u^2 - p_x^2 - p_y^2}} \\
\frac{dy}{dz} &= \frac{\partial H}{\partial p_y} = \frac{p_y}{\sqrt{u^2 - p_x^2 - p_y^2}} \\
\frac{dp_x}{dz} &= -\frac{\partial H}{\partial x} = -\frac{1}{2}\frac{1}{\sqrt{u^2 - p_x^2 - p_y^2}}\frac{\partial u^2}{\partial x} \\
\frac{dp_y}{dz} &= -\frac{\partial H}{\partial y} = -\frac{1}{2}\frac{1}{\sqrt{u^2 - p_x^2 - p_y^2}}\frac{\partial u^2}{\partial y}.
\end{aligned} \tag{6.152}$$

If the medium is only dependent on z, we find again the results of one of the previous sections. Unfortunately, one cartesian coordinate is emphasized compared to the two others and in a general heterogeneity, one would like to avoid the a-priori of selection of one coordinate. In order to do so, a new coordinate system must be introduced which is related to the sampling parameter s. This is the so-called centered ray coordinates system which is a curvilinear system used by Popov (1982) or by Červený *et al.* (1977). This system is interesting except in the complexity of the hamiltonian. Because it follows the ray, no difficulty is expected compared to the reduced hamiltonian in z. The hamiltonian is no longer constant along the ray. It must be underlined that the opposite procedure is performed in physics: when the hamiltonian for non-isolated system varies, the associated phase space is embedded inside another one where the system is isolated and the hamiltonian constant. The reason for this transformation is the expected simplicity of the extended hamiltonian. We believe that the same argument provides a strong support to the use of the complete hamiltonian (6.144) for rays.

6.9.2 *How to solve these ordinary differential equations*

Once we have defined the non-linear system to solve, we have to look for very efficient solvers because the number of rays we often need is the order of thousands and the knowledge of the medium we have is not so accurate that we need very precise and stable solvers. Moreover, the variation of velocity we find in the Earth is such that difficulties in the integration of the differential equations as stiffness problems are unexpected.

Usual solvers as Runge-Kutta or predictor-corrector schemes are suitable for tracing rays. Adaptative steps might increase the efficiency of the solver especially where the medium is homogeneous. We refer the reader to any numerical book where the details of these numerical schemes are explained. We find that a second-order Runge-Kutta is easy to program and give accurate results for most purposes in ray tracing. The description of the velocity or any equivalent field must be done through interpolating function such that at any point inside the medium we can estimate the value of the velocity as well as its first-order spatial derivatives requires for solving the O.D.E. associated with ray tracing. Often, the velocity is described by values on nodes of a grid under an explicit form $c = f(x, z)$ and a quadratic interpolation is enough to guarantee the continuity of the first-derivative. At each step of the ray tracing, we must evaluate where the ray is and what are the velocity and its derivatives at the current point of the ray. This is the main CPU time-consuming part for any computer code performing ray tracing because one must do it thousands of time. Writing a ray tracing program with initial conditions for a smooth medium is rather simple and is based on the interpolating subroutine of the velocity and its derivatives. The B-spline interpolation turns out to be an efficient way to compute smooth variation of the velocity. The first derivative is required and the B-spline of order 3, *i.e.* of degree 2, is enough. In the next section, we shall require B-splines of order 4 for estimating the amplitude. Consequently, we propose this order 4 for writing the computer code.

Another alternative is a finite element method where the medium is described by elementary cells with a simple velocity structure inside each block in order to solve analytically the equations. The task is to compute intersection points between blocks which are an order of magnitude less than for numerical solvers. Of course, the difficulty is not solved and goes to the description in blocks of the medium. Often, the description in blocks of the medium is so crude that instabilities in amplitude estimation for a given ray are found.

Finally, perturbation methods use the solution of the medium divided by blocks and construct an approximate solution which is expected to be near the one obtained by numerical methods. This intermediate solution removes instabilities in amplitude at the expense of an increase of computer time. When tracing rays becomes more complex as for anisotropic media, these perturbations techniques might be very appealing and more efficient than a dumb numerical solver although it is still an open question. For the isotropic case in a 2D medium, the ratio between a Runge-Kutta scheme and a perturbation scheme is of a factor 2.

6.10 Paraxial theory or linearization of ray tracing

Tracing rays is not enough: we need to estimate the amplitude in order to compute seismogram and also for many other aims as two-point ray tracings, caustic detections... The equation we need to solve is the transport equation. In fact, this equation is related to the ray tube which is defined by rays. Solving the transport equation leads to trace rays in the vicinity of a given selected ray. Solving directly the transport equation is not needed.

Until recently, the ray tube was estimated by tracing a nearby ray independent of the considered ray. It was a strong weakness of the ray theory because any small perturbation seen by the nearby ray and not by the true ray induced unstable behaviour of the amplitude estimation (Figure 6.35).

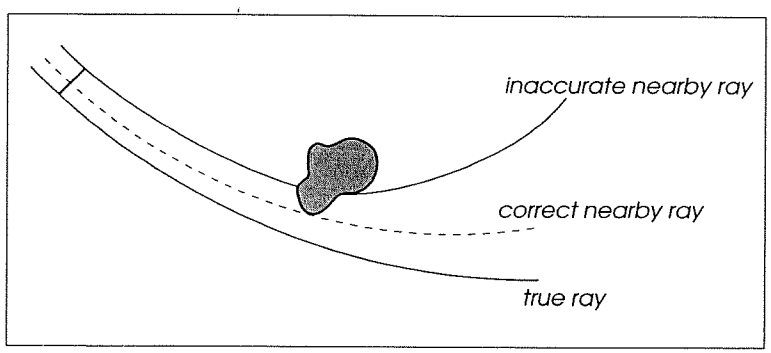

Figure 6.35 Estimation of the ray tube by nearby rays.

6.10.1 *Paraxial rays*

By a relatively distorted approach linked to gaussian beams (Červený *et al.*, 1982), seismologists go back to the elementary approach of perturbation theory (Goldstein, 1980) which computes an infinitesimal nearby ray knowing an already traced ray. This is the usual linearization approach, called paraxial theory or Gauss optics, where the reference axis is the studied ray. The linearization stabilizes the amplitude estimation because the nearby ray is only deviated by perturbations seen by the reference ray. Moreover, the linearization makes the computation very fast.

Let us assume that the nearby ray is defined by a position and a slowness vector

$$\begin{aligned} \mathbf{x}(\xi) &= \mathbf{x}_0(\xi) + \delta\mathbf{x}(\xi) \\ \mathbf{p}(\xi) &= \mathbf{p}_0(\xi) + \delta\mathbf{p}(\xi). \end{aligned} \tag{6.153}$$

The reference ray is located by $\mathbf{x}_0$ and $\mathbf{p}_0$ at parameter ξ such that

$$\begin{aligned} \frac{d\mathbf{x}_0}{d\xi} &= \nabla_{\mathbf{p}} H(\xi, \mathbf{x}_0, \mathbf{p}_0) \\ \frac{d\mathbf{p}_0}{d\xi} &= -\nabla_{\mathbf{x}} H(\xi, \mathbf{x}_0, \mathbf{p}_0) \end{aligned} \tag{6.154}$$

The following equations which must be verified by the nearby ray

$$\begin{aligned} \frac{d\mathbf{x}}{d\xi} &= \nabla_{\mathbf{p}} H(\xi, \mathbf{x}, \mathbf{p}) \\ \frac{d\mathbf{p}}{d\xi} &= -\nabla_{\mathbf{x}} H(\xi, \mathbf{x}, \mathbf{p}) \end{aligned} \tag{6.155}$$

are perturbed to first-order giving for the first equation following equalities

$$\begin{aligned} \frac{d\mathbf{x}_0}{d\xi} + \frac{d\delta\mathbf{x}}{d\xi} &= \nabla_{p_0+\delta p} H(\xi, \mathbf{x}_0 + \delta\mathbf{x}, \mathbf{p}_0 + \delta\mathbf{p}) \\ \frac{d\mathbf{x}_0}{d\xi} + \frac{d\delta\mathbf{x}}{d\xi} &= \nabla_{p_0} H(\xi, \mathbf{x}_0, \mathbf{p}_0) + \nabla_{p_0}\nabla_{p_0} H(\xi, \mathbf{x}_0, \mathbf{p}_0)\,\delta\mathbf{p} \\ &\quad + \nabla_{p_0}\nabla_{x_0} H(\xi, \mathbf{x}_0, \mathbf{p}_0)\,\delta\mathbf{x}_0 . \end{aligned} \tag{6.156}$$

Further elimination of the evolution of the reference ray provides us the linear system

$$\frac{d\delta\mathbf{x}}{d\xi} = \nabla_{p_0}\nabla_{x_0} H\,\delta\mathbf{x} + \nabla_{p_0}\nabla_{p_0} H\,\delta\mathbf{p} \tag{6.157}$$

$$\frac{d\delta\mathbf{p}}{d\xi} = -\nabla_{x_0}\nabla_{x_0} H\,\delta\mathbf{x} - \nabla_{x_0}\nabla_{p_0} H\,\delta\mathbf{p} \tag{6.158}$$

where we have dropped the subscript zero for the reference ray because confusion is no longer possible. Let us introduce the paraxial canonical ray $\delta\mathbf{y}^t = (\delta\mathbf{x}, \delta\mathbf{p})^t$ which verifies the linear system

$$\frac{d\delta\mathbf{y}}{d\xi} = A\,\delta y \tag{6.159}$$

where A is the following matrix deduced from eq. (6.157) and eq. (6.158)

$$A = \begin{pmatrix} \nabla_p \nabla_x H & \nabla_p \nabla_p H \\ -\nabla_x \nabla_x H & -\nabla_x \nabla_p H \end{pmatrix} \tag{6.160}$$

computed on the reference ray, sometimes called central ray. The nearby ray computed by this paraxial equation is only sensitive to heterogeneities felt by the reference ray, providing us a stable estimation of the ray tube. The linear system (6.159) can be solved by the propagator technique (Aki and Richards, 1980) either analytically when possible or numerically. The solution at parameter ξ is deduced from the solution at parameter ξ_0 by

$$\delta y(\xi) = \mathcal{P}(\xi, \xi_0)\, \delta y(\xi_0) \tag{6.161}$$

where $\mathcal{P}(\xi, \xi_0)$ is the propagator allowing to go from ξ_0 to ξ. From propagator theory, we have following properties

$$\frac{d\mathcal{P}}{d\xi} = A\,\mathcal{P} \quad \text{and} \quad \mathcal{P}(\xi_0, \xi_0) = I. \tag{6.162}$$

In order to distinguish what concerns the position and the slowness vector, we write the propagator in the standard form (Popov, 1982):

$$\mathcal{P}(\xi, \xi_0) = \begin{pmatrix} Q_1 & Q_2 \\ P_1 & P_2 \end{pmatrix} \tag{6.163}$$

where Q_1, Q_2, P_1, P_2 are sub-matrices whose dimensions depend on the differential system we have selected. From the Liouville theorem which states that a volume in phase space is incompressible, we have the important property of the propagator:

$$\text{Trace}\,(A) = 0 \leftrightarrow \det \mathcal{P}(\xi, \xi_0) = 1\,. \tag{6.164}$$

Other relations, often called Luneberg relations (Luneberg, 1944), coming from differential rules, are

$$\begin{aligned} Q_1 Q_2^t - Q_2 Q_1^t &= 0 \\ Q_1 P_2^t - Q_2 P_1^t &= I \\ P_1 P_2^t - P_2 P_1^t &= 0 \\ P_2 Q_1^t - P_1 Q_2^t &= I \end{aligned} \tag{6.165}$$

which implies immediately (6.164) as well as the inverse propagator

$$P^{-1} = \begin{pmatrix} P_2^t & -Q_2^t \\ -P_1^t & Q_1^t \end{pmatrix}. \tag{6.166}$$

Each submatrix is obtained by solving the propagator for particular initial conditions. By assuming $\delta y(\xi_0)^t = [I\ 0]$, we obtain submatrices Q_1 and P_1, while $\delta y(\xi_0)^t = [0\ I]$ gives the two other submatrices Q_2 and P_2. The linear combination of these solutions is also a solution.

In a two-dimensional medium with cartesian coordinate system, we may define four elementary solutions with initial paraxial canonical vector equal to zero except for one component δx or δz or δp_{x0} or δp_{z0} shown in Figure 6.36. General solutions are obtained by linear combination but they are not paraxial rays: to be a paraxial ray, they must verify the additional equation

$$\delta H = \nabla_x H\, \delta \mathbf{x} + \nabla_p H\, \delta \mathbf{p} = 0 \tag{6.167}$$

which means that $\nabla_x H\ \delta \mathbf{x} = 0$ when $\delta \mathbf{p} = 0$ and $\nabla_p H\ \delta \mathbf{p} = 0$ when $\delta \mathbf{x} = 0$. Generally, elementary solutions are not paraxial rays. The Jacobian J_{2D} can be estimated with two elementary solutions. These solutions are associated with $\delta p_x = 1$, denoted by subscript 3 and $\delta p_z = 1$, denoted by subscript 4, initial conditions. The Jacobian is obtained through the determinant

$$J_{2D} = \begin{vmatrix} p_x & \delta x_3 & \delta x_4 \\ p_z & \delta z_3 & \delta z_4 \\ 0 & p_{xi} & p_{zi} \end{vmatrix}. \tag{6.168}$$

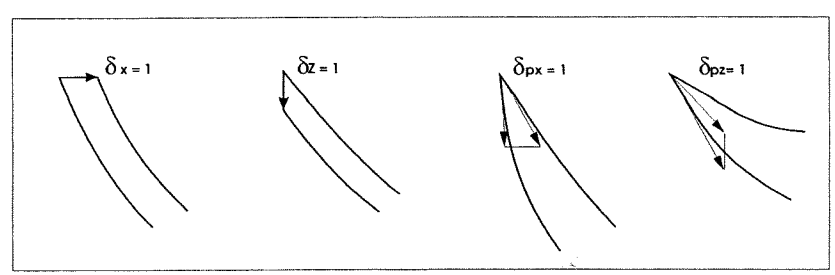

Figure 6.36 Geometrical illustration of elementary trajectories for a 2D medium: they are not rays.

Figure 6.37 shows the elementary solution for an initial slowness perturbation along x as well as the elemetary solution for an initial slowness perturbation along z. The paraxial ray is also estimated in this figure and is used for the Jacobian computation.

It is very important to stress that the paraxial solution is always coordinate-dependent and that coordinate transformations provide other paraxial approximations. Only when coordinate transformations are linear, can an equivalence between paraxial solutions be obtained. In particular, this is true between ray-centered and local cartesian coordinate systems (Červený, 1985) but it is not true for non-linear transformation as proposed by Virieux and Ekström (1991).

Let us consider a vertical dependence of the velocity: the reduced hamiltonian

$$\mathcal{H}(z, x, p_x) = -\sqrt{u^2(z) - p_x^2} \tag{6.169}$$

is selected for a ray pointing downward. We find the following linear differential system

$$\frac{d\delta \mathbf{y}}{dz} = \begin{pmatrix} 0 & u^2/(u^2 - p_x^2)^{3/2} \\ 0 & 0 \end{pmatrix} \tag{6.170}$$

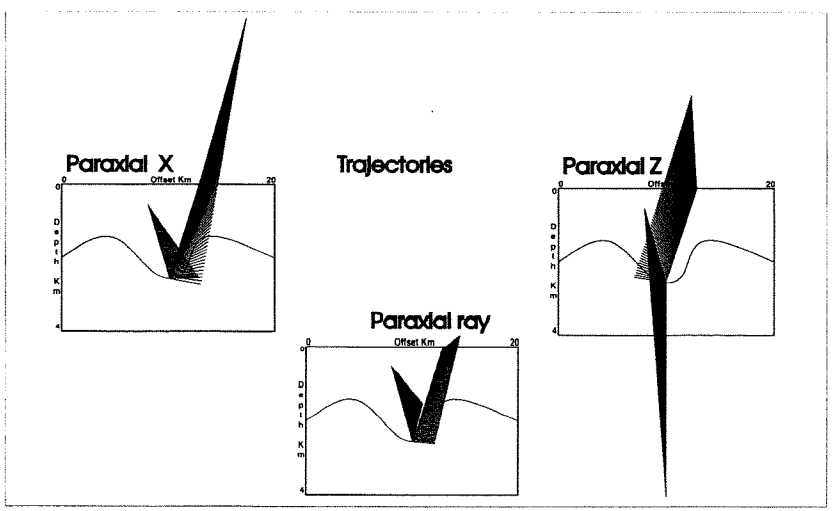

Figure 6.37 Paraxial trajectories as well as paraxial ray is drawn with an a-priori finite amplitude. Only the space component of the paraxial vector is presented. The left panel is for an initial condition along x; the right panel is for an initial condition along z and the middle panel is the paraxial ray.

which leads to a quadrature for the paraxial canonical vector

$$\delta p_x(z) = \delta p_x(z_0)$$

$$\delta x(z) = \delta x(z_0) + \delta p_x(z_0) \int_{z_0}^{z} \frac{u^2}{(u^2 - p_x^2)^{3/2}}\, dz \tag{6.171}$$

and a simple expression for the propagator

$$\mathcal{P} = \begin{pmatrix} 1 & Q_2 \\ 0 & 1 \end{pmatrix}. \tag{6.172}$$

The term Q_2 identified by relation (6.171) is related to the position X (eq. 6.122) by

$$Q_2 = \frac{dX}{dp_x} = \frac{d}{dp_x} \int_{z_0}^{z} \frac{p_x}{\sqrt{u^2 - p_x^2}}\, dz \tag{6.173}$$

which is linked to the Jacobian estimation (6.109).

For a constant gradient of the square of slowness, it is a trivial matter to obtain the propagator as

$$\begin{pmatrix} 1 & (\tau - \tau_0) \\ 0 & 1 \end{pmatrix} \tag{6.174}$$

which gives the term Q_2 equivalent to the eq. (6.174).

For the general case, we must use previously mentioned methods for ray tracing as numerical solvers, but the linearity allows one to integrate with a rather important sampling parameter. The effort for computing many elementary solutions is the same as the one for one elementary solution because we need partial derivatives of the hamiltonian along the central ray which is the most time-consuming effort and which is performed only once. Because eq. (6.159) requires second-order derivatives, we estimate velocity and its phase-space derivatives with B-splines of order 4. Only few FORTRAN extra lines are required to solve the paraxial ray tracing problem simultaneously as the ray tracing problem when the current position of the ray is known. This is only true for smooth media. We shall see that interface makes ray tracing more complex as well as paraxial ray tracing.

6.10.2 *Beams of rays*

Tracing paraxial rays with random initial conditions will sample the whole space: we must select initial conditions in order to observe a plane wave or waves

emitted by a point source. By a proper choice of initial conditions, we define a beam of paraxial rays. In order to preserve the linearity of solutions, we define initial conditions as a hyperplane in phase space,

$$a\,\delta\mathbf{p}\,(\xi_0)+b\,\delta\mathbf{x}\,(\xi_0)=0 \tag{6.175}$$

which often is written in the following form

$$\delta\mathbf{x}\,(\xi_0)=\epsilon\,\delta\mathbf{p}\,(\xi_0) \tag{6.176}$$

with a possible infinite value for ϵ. When $\epsilon=0$, we have the point source condition and when $\epsilon=\infty$, we have the plane wave conditions. From eq. (6.161) and eq. (6.176), a linear relation between paraxial position and paraxial slowness vector

$$\delta\mathbf{p}\,(\xi)=\mathcal{M}\,(\xi)\,\delta\mathbf{x}\,(\xi) \tag{6.177}$$

introduces the matrix

$$\mathcal{M}\,(\xi)=\epsilon Q_1+Q_2^{-1}\epsilon P_1+P_2 \tag{6.178}$$

which is related to the curvature of the local wavefront (Popov, 1982). In a two-dimensional medium, we have the radius of curvature $\mathcal{R}$ equal to

$$\mathcal{R}=\frac{\delta n}{\delta\theta}=\frac{u\,\delta n}{\delta p_n}=u\,(\xi)\,\frac{1}{\mathcal{M}\,(\xi)} \tag{6.179}$$

as shown by Figure 6.13. The curvature,

$$\mathcal{K}=c\,(\xi)\,\mathcal{M}\,(\xi), \tag{6.180}$$

is therefore directly proportional to matrix $\mathcal{M}$ which justifies the notation. Finally, the continuity of the wavefront deduced from the paraxial theory is related to the spatial derivatives of the travel-time, information which is important in different applications as earthquake locations or travel-time interpolations.

One might quote the different applications of the paraxial theory. The first application is the estimation of the jacobian and, consequently, the amplitude evaluation. The elementary surface dS' is given by

$$dS'\,(\xi)=\det\,(\epsilon Q_1+Q_2)\,\frac{\sin\theta}{\sin\theta_0}\,dS'\,(\xi_0) \tag{6.181}$$

where θ is the angle between the slowness vector and the paraxial position as shown in Figure (6.38). We have the following simple interpretation of the

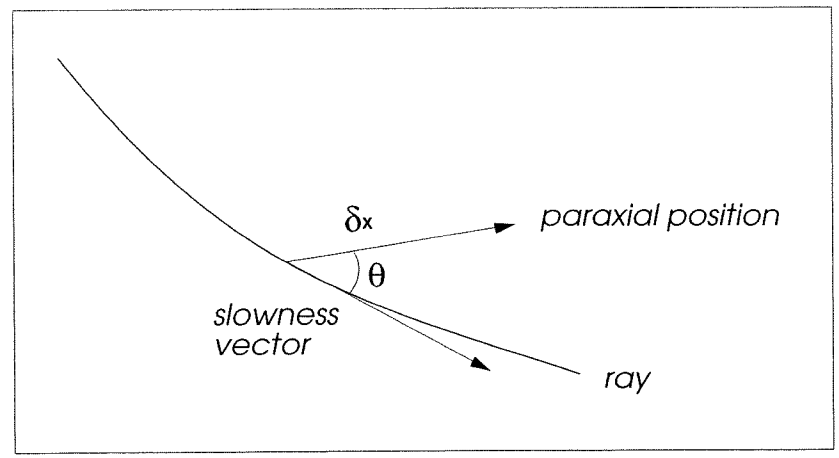

Figure 6.38 Geometry of paraxial ray: the paraxial position as well as the paraxial slowness vector define the paraxial vector. Jacobian and amplitude can be deduced from the paraxial ray.

geometrical spreading of a plane wave with Q_1 and the geometrical spreading of a point source with Q_2. Another application is the estimation of travel-time under a parabolic approximation through the formula

$$T(\mathbf{x}+\delta\mathbf{x})=T(\mathbf{x})+\mathbf{p}\cdot\delta\mathbf{x}+\frac{1}{2}\,\delta\mathbf{x}'\,\mathcal{M}\delta\mathbf{x}. \tag{6.182}$$

Finally, the estimation of geometrical spreading allows by iteration to shoot at a given station by a Newton method. The two-point ray tracing problem can be solved locally.

In partial conclusion, one can say that this paraxial theory is a rather classical section of mechanical (Goldstein, 1980) or optical textbooks (Born and Wolf, 1986) and has been recently rediscovered by seismologists with the complexity of the heterogeneity we have in the Earth. The use of centered ray coordinates system is not required by this theory and is only a known way to reduce the number of variables and equations.

6.11 Vector high frequency approximation

Until now, we have focused our attention on the scalar acoustic equation, stating that the elastic case is not very different. We shall discuss here the high frequency solution for the elastic case (Červený *et al.*, 1977). We start from a similar

ansatz of the solution

$$u(\mathbf{x}, \omega) = S(\omega)\,\mathbf{A}(\mathbf{x}, \omega)\,e^{i\omega T(\mathbf{x})} \tag{6.183}$$

where the amplitude term is a vector. A series in inverse powers of ω is assumed for this vector

$$\mathbf{A}(\mathbf{x}\omega) = \sum_k \frac{\mathbf{A}^k(\mathbf{x})}{(-i\omega)^k} \tag{6.184}$$

and is inserted in the elastodynamic equation

$$(C_{ijkl}u_{k,l})_{,j} + f_i = \rho u_{i,tt} \tag{6.185}$$

for an anisotropic medium. We consider an anistropic medium simply because the elastodynamic equation has a compact form. Arranging eq. (6.185) in powers of ω we find a cascade of equations. The term in ω^2 gives the following equation

$$C_{ijkl}T_{,j}T_{,l}A_k^0 - \rho A_i^0 = 0 \tag{6.186}$$

which can be written as a relatively simple equation

$$\Gamma_{ik}A_k^0 - A_i^0 = 0 \tag{6.187}$$

with

$$\Gamma_{ik} = \frac{C_{ijkl}T_{,j}T_{,l}}{\rho}. \tag{6.188}$$

The matrix Γ is called the elastodynamic matrix of the ray theory and has very interesting properties which we do not discuss here as they have no direct applications in the following.

Let us look for a non-zero solution of (6.187) and, consequently, for the eigenvalues G_m and eigenvectors g_m of eq. (6.187). The eigenvalues G_m are defined by setting the following determinant

$$D = \det(\Gamma_{ik} - G_i\delta_{ik}) \tag{6.189}$$

equal to zero. After a tedious manipulation, one can factor the determinant into two terms

$$D = \left(\frac{\mu}{\rho}T_{,i}T_{,i} - G_m\right)^2\left(\frac{\lambda+2\mu}{\rho}T_{,i}T_{,i} - G_m\right) \tag{6.190}$$

for an isotropic medium. We find two eigenvalues one of which has a double degeneracy. The associated eigenvectors verify the following equations

$$(\Gamma_{ik} - G_m\delta_{ik})\,g_k^m = 0. \tag{6.191}$$

The eigenvector $\mathbf{g}^3$ is associated with the single eigenvalue and is orthogonal to the two others $\mathbf{g}^1$ and $\mathbf{g}^2$ which can not be determined uniquely. The degeneracy of the second eigenvalue determines only the plane where they are lying. Let us denote two quantities with a notation which will be understood in a moment

$$\alpha = \frac{\lambda+2\mu}{\rho}$$

$$\beta = \frac{\mu}{\rho}. \tag{6.192}$$

Equation (6.187) requires eigenvalues equal to the unity which implies one of the two following equations

$$T_{,i}T_{,i} = \frac{1}{\alpha^2}$$

$$T_{,i}T_{,i} = \frac{1}{\beta^2} \tag{6.193}$$

which show that α and β are local phase velocities and that eqs. (6.193) are identical to the eikonal for the acoustic case. In other words, solving eikonal equations for the elastic case is the same as solving eikonal equations for the acoustic case.

For polarizations, the situation is slightly more complex and requires explicitly the isotropic case for eq. (6.186). We have

$$\frac{\lambda+2\mu}{\rho}\nabla T(\nabla T\cdot\mathbf{A}^0) + \frac{\mu}{\rho}(\nabla T)^2\mathbf{A}^0 - \mathbf{A}^0 = 0 \tag{6.194}$$

which gives the following equations by taking the scalar and cross products:

$$(\alpha^2(\nabla T)^2 - 1)(\mathbf{A}^0\cdot\nabla T) = 0$$

$$(\beta^2(\nabla T)^2 - 1)(\mathbf{A}^0\cdot\nabla T) = 0 \tag{6.195}$$

For waves propagating at speed α, the following equation

$$\mathbf{A}^0\times\nabla T = 0 \tag{6.196}$$

should be verified and demonstrates that we have compressive waves called P waves parallel to ∇T or slowness vector $\mathbf{p}$. The amplitude is linearly polarized perpendicular to the wavefront

$$\mathbf{A}^0 = A_3\, \mathbf{g}^3. \tag{6.197}$$

For waves propagating at speed β, the following equation

$$\mathbf{A}^0 \cdot \nabla T = 0 \tag{6.198}$$

shows that the motion is perpendicular to the slowness vector and creates a shear wave called S waves. The amplitude is elliptically polarized from the general expression

$$\mathbf{A}^0 = A_1\, \mathbf{g}^1 + A_2\, \mathbf{g}^2. \tag{6.199}$$

Figure 6.39 summarizes the polarization of the two kinds of waves. The expression for the P-wave displacement in the frequency domain is

$$\mathbf{u}(\mathbf{x}, \omega) = S(\omega)\, \mathbf{t}\, A_3(\mathbf{x})\, e^{i\omega T_p(\mathbf{x})} \tag{6.200}$$

with an amplitude proportionnal to $1/\sqrt{\alpha\rho|J|}$. By going back to the time domain, we find a similar solution to the acoustic case

$$\mathbf{u}(\mathbf{x}, t) = \mathbf{t}\, \phi_3(\gamma_1, \gamma_2)\, \mathcal{R}\left\{ \frac{1}{\sqrt{\alpha\rho J}}\, \tilde{S}(t - T_p(\mathbf{x})) \right\}. \tag{6.201}$$

For S waves, an arbitrary selection of eigenvectors $\mathbf{g}_1$ and $\mathbf{g}_2$ leads to a coupling between the propagation of amplitude A_1 and amplitude A_2. For a specific set of eigenvectors such that

$$\frac{d\mathbf{g}^1}{ds} \propto \mathbf{t}$$

$$\frac{d\mathbf{g}^2}{ds} \propto \mathbf{t} \tag{6.202}$$

we obtain an independent propagation for quantities A_1 and A_2. These particular vectors, denoted $\mathbf{e}_1$ and $\mathbf{e}_2$, are those of the ray-centered coordinates system (Figure 6.40) which provides a simple description of the propagation with a decoupling between A_1 and A_2. I think this is the most important contribution of this particular coordinate system. The S-wave displacement is given finally in the

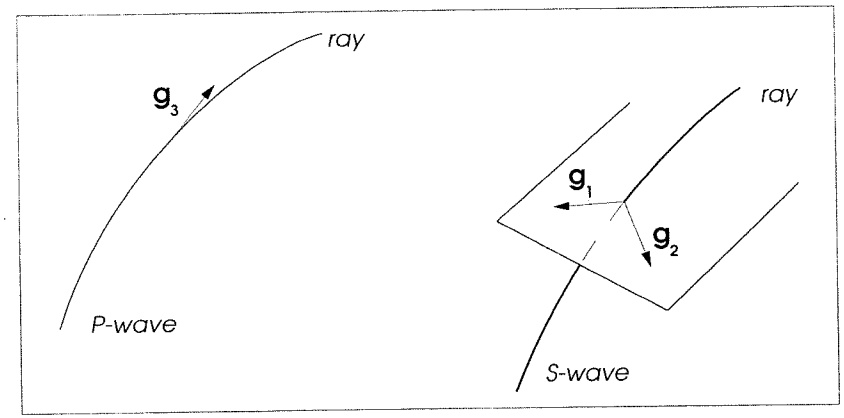

Figure 6.39 Polarization vectors in a 3D medium.

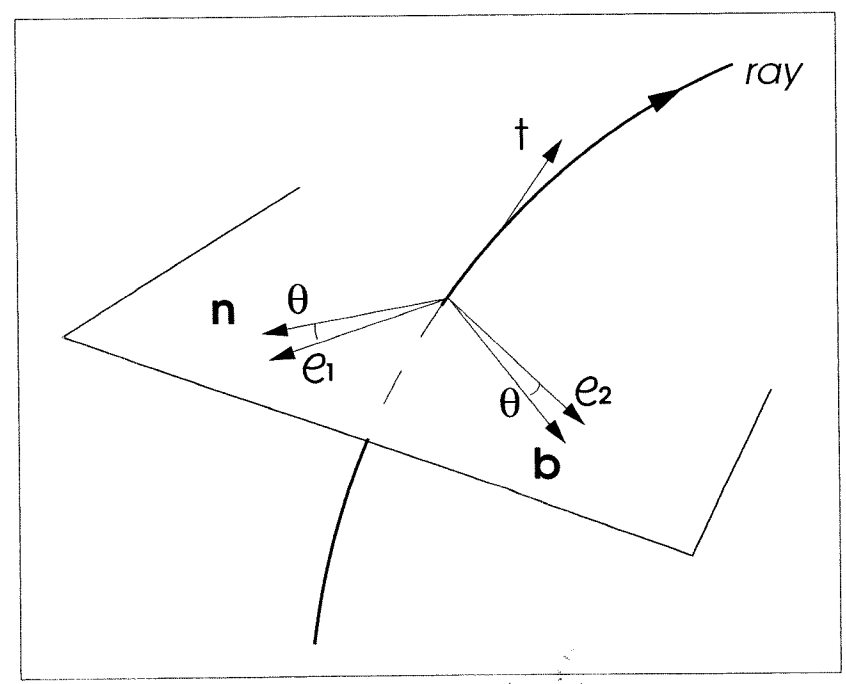

Figure 6.40 Geometrical relation between Frénet vectors and ray-centered coordinate system.

time domain by

$$\mathbf{u}(\mathbf{x}, t) = \mathbf{e}_1 \phi_1(\gamma_1, \gamma_2) \mathcal{R}\left\{\frac{1}{\sqrt{\beta \rho J}} \tilde{S}(t - T_s(\mathbf{x}))\right\}$$

$$+ \mathbf{e}_2 \phi_2(\gamma_1, \gamma_2) \mathcal{R}\left\{\frac{1}{\sqrt{\beta \rho J}} \tilde{S}(t - T_s(\mathbf{x}))\right\}. \tag{6.203}$$

We must follow the evolution of the vectors $\mathbf{e}_1$ and $\mathbf{e}_2$ during the propagation. This is the only added difficulty compared with the acoustic case, a remarkable result of the ray theory.

6.12 Interfaces

6.12.1 *Discontinuity of first order*

High frequency propagation assumes a smooth variation of physical properties of the medium, while in the Earth sharp boundaries are often met. If the boundary is sharp enough in order to avoid any effect of a length scale, we can still apply the ray theory from one side to the other one of the discontinuity and check explicitly the "continuity" of the solution along the interface.

Starting with an incident wave denoted with subscript i, a reflected wave denoted with subscript r and a transmitted wave denoted with subscript t are generated at the interface position. The continuity of the phase of the wave field and the invariance with respect to time implies the equality of travel-times:

$$T_i = T_r = T_t, \tag{6.204}$$

while the spatial tangential invariance along the interface implies the following equality

$$\mathbf{n} \times \nabla_{\mathbf{x}} T_i = \mathbf{n} \times \nabla_{\mathbf{x}} T_r = \mathbf{n} \times \nabla_{\mathbf{x}} T_t \tag{6.205}$$

which is known to be the Snell-Descartes law. At the same time, we must require the continuity of displacements and stresses along the interface. We must evaluate the surface of ray tube intersected by the interface for the three kinds of rays as well as reflection and transmission coefficients. The incident pressure at position $\mathbf{x}_I$ on the interface

$$P_i(\mathbf{x}_I, \omega) = S(\omega) \phi(\gamma_1, \gamma_2) \sqrt{\frac{1}{u(\mathbf{x}_I)|J_i(\mathbf{x}_I)|}}\, e^{i\omega T_i(\mathbf{x}_I)}\, e^{-i\frac{\pi}{2}\mathrm{KMAH}} \tag{6.206}$$

generates reflected pressure at position $\mathbf{x}$

$$P_r(x, \omega) = S(\omega) \phi(\gamma_1, \gamma_2) R \sqrt{\frac{|J_r(\mathbf{x}_I)|}{|J_i(\mathbf{x}_I)|}} \sqrt{\frac{1}{u(\mathbf{x})|J_r(\mathbf{x})|}}\, e^{i\omega T_r(\mathbf{x})}\, e^{-i\frac{\pi}{2}\mathrm{KMAH}} \tag{6.207}$$

as well as transmitted pressure

$$P_t(x, \omega) = S(\omega) \phi(\gamma_1, \gamma_2) T \sqrt{\frac{u_t(\mathbf{x}_I)|J_t(\mathbf{x}_I)|}{u(\mathbf{x}_I)|J_i(\mathbf{x}_I)|}} \sqrt{\frac{1}{u(\mathbf{x})|J_t(\mathbf{x})|}}\, e^{i\omega T_t(\mathbf{x})}\, e^{-i\frac{\pi}{2}\mathrm{KMAH}}. \tag{6.208}$$

Denoting θ_i the angle between the normal at the interface and the slowness vector of the incident field at the hitting point as well as the angle θ_r for reflected fields and the angle θ_t for transmitted fields (Figure 6.41), we found geometrically

$$\begin{aligned} J_r(\mathbf{x}_I) &= -J_i(\mathbf{x}_I) \\ J_t(\mathbf{x}_I) &= J_I(\mathbf{x}_I) \cos\theta_t \\ J_i(\mathbf{x}_I) &= J_I(\mathbf{x}_I) \cos\theta_i \end{aligned} \tag{6.209}$$

and the continuity of the energy implies that J_I is continuous which means

$$\frac{J_t}{\cos\theta_t} = \frac{J_i}{\cos\theta_i}. \tag{6.210}$$

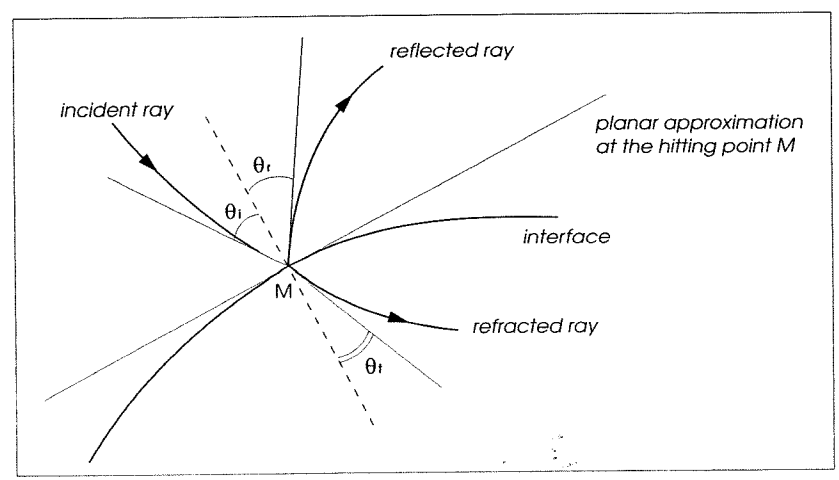

Figure 6.41 Geometry of rays at the interface between two media.

The reflected and transmitted coefficients R and T are those for plane waves hitting a planar interface as a valid approximation at the high frequency we are looking (Figure 6.41). Incorporating the effect of geometrical spreading in the coefficients published in the literature (Červený *et al.*, 1977; Aki and Richards, 1980), we found extended coefficients proposed by Červený (personal communication)

$$t = T\sqrt{\frac{u_t(\mathbf{x}_I)|\cos\theta_t|}{u_i(\mathbf{x}_I)|\cos\theta_i|}}$$

$$r = R. \tag{6.211}$$

The final solution for a ray which has undertaken different conversions at interfaces is

$$P(x,\omega) = S(\omega)\,\phi(\gamma_1,\gamma_2)\,\Pi\sqrt{\frac{1}{u(\mathbf{x})|J(\mathbf{x})|}}\;e^{i\omega T_i(\mathbf{x})}\,e^{-i\frac{\pi}{2}\mathrm{KMAH}}, \tag{6.212}$$

where Π is the product of extended coefficients r and t along the ray. For the displacement, we have to modify slightly the final formula as shown in the elastic approach and we get

$$t = T\sqrt{\frac{\rho_t u_t(\mathbf{x}_I)|\cos\theta_t|}{\rho_i u_i(\mathbf{x}_I)|\cos\theta_i|}}$$

$$r = R \tag{6.213}$$

as well as the displacement

$$u(x,\omega) = S(\omega)\,\phi(\gamma_1,\gamma_2)\,\Pi\sqrt{\frac{1}{\rho(\mathbf{x})c(\mathbf{x})|J(\mathbf{x})|}}\;e^{i\omega T_i(\mathbf{x})}\,e^{-i\frac{\pi}{2}\mathrm{KMAH}}. \tag{6.214}$$

Finally, the ray theory is valid for smooth variation of reflection coefficients and the interface curvature. Different strategies must be used when these properties are not fulfilled as we have seen in a previous section.

6.12.2 *Boundary conditions for paraxial rays*

Once we have solved continuity conditions for the ray we must know how the paraxial ray is converted through an interface. In other words, we must know how the evolution of the ray tube is modified by the interface, which is a more difficult problem than estimating the ray tube intersection with the interface.

A complete discussion is beyond the purpose of this course. Let us underline that the Hamiltonian formalism has been useful to construct the connecting formula as shown by Farra *et al.* (1989), while the previous analysis by Červený *et al.* (1974) was performed by pure differential geometry operators. Whatever the way we construct this transformation, it must be a local linear transformation expressed by a matrix.

The new paraxial vectors $\delta y'$ is obtained in the new medium through a linear relation with the paraxial vector δy of the incident medium. Basically two transformations are required. The first operation is a projection Π along the slowness vector of the reference ray of the paraxial vector on the interface. Then a second operation, denoted $\mathbf{T}$, must be performed and involves the curvature of the interface at the hitting point of the reference ray. This term is difficult to estimate because media on each side of the interface can be heterogeneous, a situation found only in seismology. Figure 6.42 summarizes the different transformations to allow

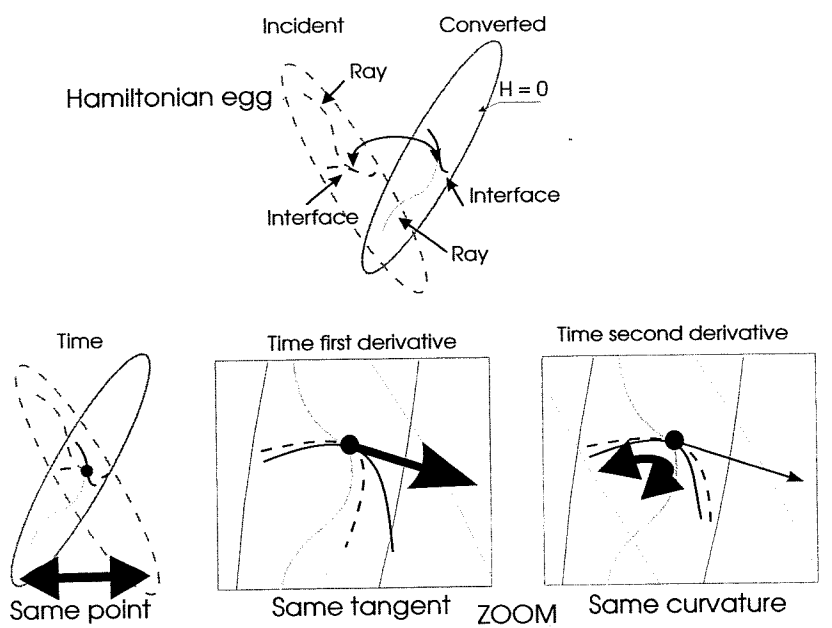

Figure 6.42 Schematic interpretaion of boundary conditions at an interface for both rays and paraxial vectors. The top panel shows the incident and converted hypersurfaces of each Hamiltonian equal to zero. These hypersurfaces are completely disconnected. The continuity of travel-time connects the two hypersurfaces as one can seen in the left of the bottom panel. The continuity of travel-time first-derivative requires the first "rotation" of one hypersurface with respect to the other (middle figure of the bottom panel) and the continuity of travel-time second-derivative requires the second "rotation" (right figure of the bottom panel).

a ray to be converted at an interface: a) the continuity of the time associated with a translation of the incident and converted Hamiltonians at the intersecting point, b) the continuity of the first derivative equivalent to the Snell law which implies the first rotation of the Hamiltonians, c) the continuity of the second derivative which implies the transformation between paraxial vectors.

6.12.3 *Topology between interfaces and surrounding media*

When solving ray tracing equations, we must always face the same problem which is to know where is the ray position at each step of integration. The problem is now more difficult because the ray might have hit an interface and might go into another medium. Therefore, we must provide a link between the description of the different media and the description of interfaces. Basically, one interface separates two media. This additional information about the topology of interfaces and media must be provided to the ray tracing solver. Also, the different conversions of the ray on interfaces must be defined. This is achieved through a signature saying into which media the ray is going through. A more global strategy is to

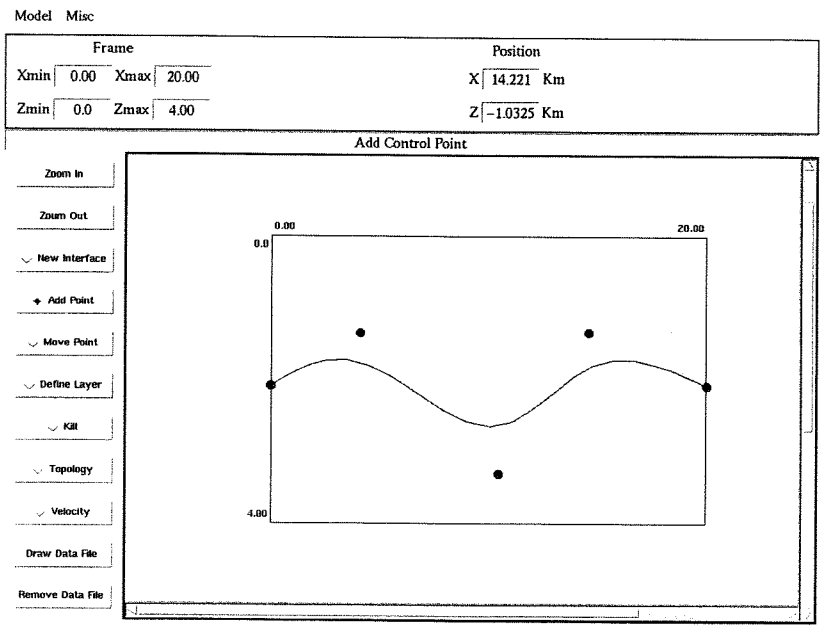

Figure 6.43 Interface representation shown in a computer frame to define complex 2D models.

assign a given type of conversion at a given interface and to let rays bouncing on these interfaces until they reach the free surface.

It is worth mentioning that, whatever is the sophisticated formulation of ray theory, the efficiency of a ray tracing code is linked to the efficiency of analyzing the new estimated point of the ray. Many strategies exist and some of them have been borrowed from graphical software or from image synthetics. For example, instead of looking for an intersection with interfaces surrounding the current medium where is the ray, we might look at intersections with simple basic volumes/surfaces enveloping the interfaces. If the intersection is obtained, we must go one step further and check the intersection with the interface itself. If not, we have saved our time for an intersection search with a complex object as an arbitrary interface (Virieux and Farra, 1991). Figure 6.43 shows an interface defined through B-spline interpolation, with control points which attract the interface curve. Because the B-spline is of order 4, three points are needed to make the curve going through the control point. Of course, discontinuity in curvature or in slope is possible by handling carefully a multiplicity of control points.

6.13 Synthetic seismograms

6.13.1 *Difficulties of ray seismograms*

We have seen that, once one knows the ray arriving at a station, evaluating synthetic seismograms is a simple matter in the framework of the ray theory. The signal at the station is the contribution along the ray of an infinitely thin portion of the medium. Constructing this line is a time-consuming task and missing a ray is always possible. This is a weakness of the ray theory.

For finite frequencies, we expect singularities to be smoothed out by diffusion: other areas of the medium not crossed by rays contribute to seismograms (Chapman and Orcutt, 1985).

An intermediate approach between full wave propagation (Aki and Richards, 1980) and high frequency approximation of the ray theory has been proposed by Chapman (1978) and has its root in spectral methods. The basic idea is to propose a contribution of rays propagating into the medium even if they do not reach the station.

6.13.2 *WKBJ seismograms*

Let us start with a two-dimensional homogeneous medium of speed c. The pressure P in the spectral domain is given by

$$P(\mathbf{x}, \omega) = \frac{i}{4} H_0^1\left(\frac{\omega r}{c}\right). \tag{6.215}$$

The Hankel function is decomposed into exponential functions which gives the Weyl integral

$$P(\mathbf{x}, \omega) = \frac{i}{4\pi} \int_{-\infty}^{\infty} e^{i\omega(px+qz)} \frac{dp}{q} \tag{6.216}$$

where

$$q^2 + p^2 = \frac{1}{c^2} \tag{6.217}$$

for positive frequency ω and positive coordinate z. The quantity q needed in the integral 6.216 requires the definition of the square root: we select q such that $Im\,(q) > 0$ in order to have a damping of waves when z is positive. When the square root is real, eq. 6.216 is a decomposition in plane waves and, when the square root is complex, we have contribution of inhomogeneous waves (Figure 6.44).

The solution in the time domain

$$P(\mathbf{x}, t) = \frac{1}{4\pi^2} \int_{-\infty}^{\infty} d\omega \int_{-\infty}^{\infty} e^{i\omega(px+qz-t)} \frac{i}{2} \frac{dp}{q} \tag{6.218}$$

can be evaluated either by integrating on p before integrating on ω – reflectivity method (real p) and full wave theory (complex p) – or by integrating first on ω and then on p – generalized ray method (complex p) or WKBJ method (real p). The last method has a simple physical interpretation related to rays and we describe it now.

Changing the integration variable from p to angle θ by

$$p = \frac{\sin\theta}{c} \quad \text{and} \quad q = \frac{\cos\theta}{c} \tag{6.219}$$

simplify even more eq. 6.218

$$P(\mathbf{x}, t) = \frac{1}{4\pi^2} \int d\omega \int_L e^{i\omega(T-t)} \frac{i}{2} d\theta. \tag{6.220}$$

The contour L is given by Figure 6.45 where angle θ has imaginary components. Integration is often along the real axis. Oher contours are possible: the full wave theory (Aki and Richards, 1980) select the complex Cagniard path to estimate the solution. The travel-time $T = \mathbf{p} \cdot \mathbf{x}$ is the travel-time of a plane wave with a direction $\mathbf{p}$. This equation is exact with inhomogeneous waves along the z axis. These waves which are important near the source are often neglected at high frequency.

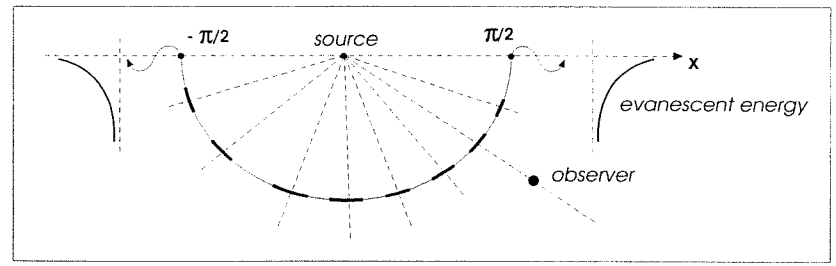

Figure 6.44 Summation of plane waves (progressive and evanescent waves) for a seismogram at the observer.

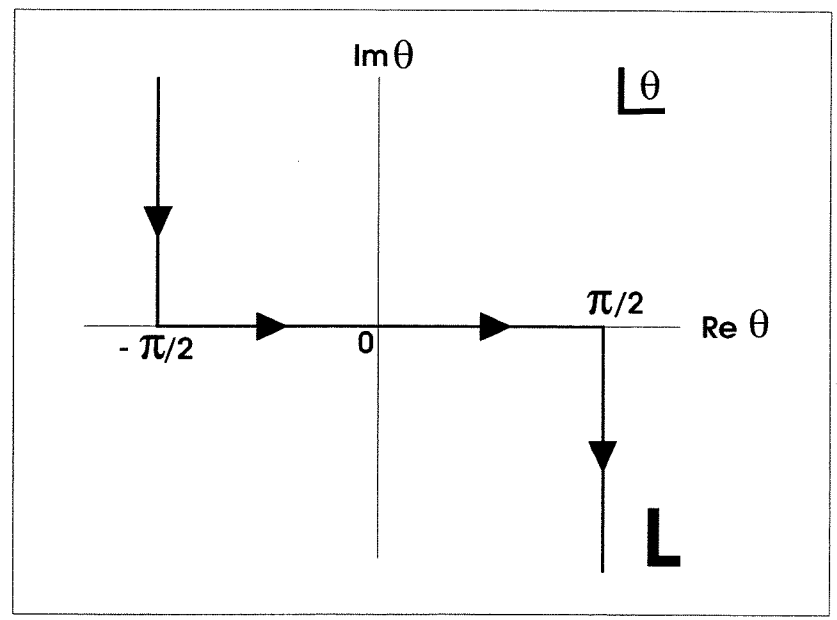

Figure 6.45 Integration path over the complex angle θ.

Moreover, the principal contribution of the oscillating exponential term comes from the saddle point where the oscillation is the smallest. This saddle point is given by

$$\frac{\partial T}{\partial \theta} = \frac{1}{c}(x\cos\theta - z\sin\theta) \tag{6.221}$$

which gives the angle of the geometrical ray arriving at the station (Figure 6.46)

$$\tan(\theta_G) = \frac{x}{z} \tag{6.222}$$

and a contribution to the pressure from the saddle point approximation

$$\frac{1}{4\pi}\sqrt{\frac{2c}{r}}\frac{H\left(t-\frac{r}{c}\right)}{\sqrt{t-\frac{r}{c}}} \tag{6.223}$$

equal to the high frequency approximation computed previously. We extend the integral evaluation on the real contour of L and obtain by integration on ω

$$P(\mathbf{x}, t) = \frac{1}{4\pi^2}\mathcal{R}\left[\int_{-\frac{\pi}{2}}^{\frac{\pi}{2}}\frac{1}{t-T(\theta)}\,d\theta\right]. \tag{6.224}$$

This integral has contribution of many angles corresponding different rays and has a singularity in $t = T$ which is removed by an adequate smoothing: a small imaginary part (often equal to $i\Delta t$ where Δt is the time sampling) is added to the travel-time T. The missing segments of contour L induce cut-off phases because plane waves have equal importance in their contribution to the pressure, but the approximation is better than taking only the geometrical arrival which need not to be calculated: two-point ray tracing is avoided.

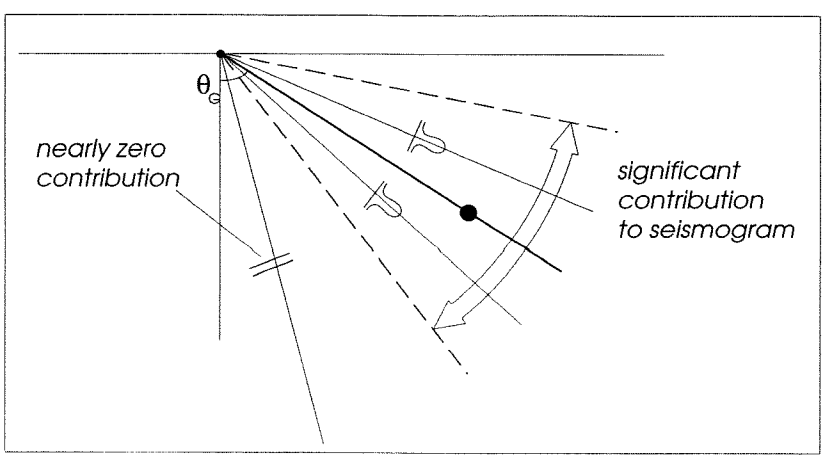

Figure 6.46 Summation of gaussian waves.

The extension in a medium with arbitrary vertical variation of the velocity is straigthforward and one obtains

$$P(\mathbf{x}, t) = \frac{1}{4\pi^2}\mathcal{R}\int_L \sqrt{\frac{q(z_0, p)}{q(z, p)}}\frac{d\theta}{t-T(p, z, x)} \tag{6.225}$$

where q is now depending in z and the travel-time $T(p, z, x)$ is the sum of the travel-time of the ray reaching the depth z and the horizontal travel-time between x and the position of the ray $X(p, z)$ as shown in Figure 6.46, *i.e.*

$$T(p, z, x) = T(p, z) + p(x - X(p, z)). \tag{6.226}$$

The procedure to compute pressure P is done in three steps: 1) decomposition of the source in Snell waves (decomposition in p), 2) propagation of each Snell wave and 3) summation at the station of the different Snell waves with the travel-time T and the geometrical spreading $1/\sqrt{q}$. An extension of the method, called Maslov method, allows to consider laterally variable medium.

The cut-off phases coming from neglecting inhomogeneous waves are the main drawback of this approach. It has been proposed to evaluate asymptotically these branches. Another technique is to make negligable the contribution of these branches by deforming the plane wave decomposition in order to have more local decomposition around the geometrical arrival. Finally, other approximations of the path integral are possible and the *WKM* method mentioned by Helmberger (1996, this issue) is a slight investigation in the complex p plane to reduce these cut-off phases.

6.13.3 *Gaussian beam summation*

The geometrical spreading in a vertically varying medium without interfaces is given by

$$q(z, p) = \frac{\cos\theta}{c(z)}Q_1 \tag{6.227}$$

for a plane wave. We write the decomposition (6.225) in a more explicit expression

$$P(\mathbf{x}, t) = \frac{1}{4\pi^2}\mathcal{R}\int_L \sqrt{\frac{c(z)\cos\theta_0}{c(z_0)\cos\theta Q_1}}\frac{d\theta}{t-T(p, z, x)} \tag{6.228}$$

and generalize the factor Q_1 to a factor Q which includes the effect of the plane wave as well as the effect of the point source. The geometrical spreading can be defined by

$$Q = Q_1 + \epsilon^{-1} Q_2 \tag{6.229}$$

as seen in the paraxial theory section: the plane wave with a zero curvature of the wavefront is deformed into a wave with a curvature $\mathcal{M}$ given by

$$\mathcal{M} = \frac{P_1 + \epsilon^{-1} P_2}{Q_1 + \epsilon^{-1} Q_2} \tag{6.230}$$

and related to a wavefront defined by

$$T(p, x, z) = T(p, z) + p\,(x - X(p, z)) + \frac{1}{2}[x - X(p, z)]^t\, \mathcal{M}\, [x - X(p, z)]. \tag{6.231}$$

The good selection of ϵ is still an open question (White *et al.*, 1988; Weber, 1988) and is related to the completeness of the decomposition of the pressure in these local waves. For a fixed arbitrary error in the initial pressure, a decomposition in gaussian waves can be performed. For Gaussian Beam Summation, the parameter ϵ is complex, while, for the Maslov method, the parameter ϵ is real. Moreover, for the Maslov method, the parameter ϵ is such that one obtains plane waves at the receiver.

These extensions of the ray theory for synthetizing seismograms have participated to the renewal of the ray theory in seismology and have increased their domain of application.

6.14 Conclusions

The ray theory allows many interpretations of propagation inside the Earth. In these notes, we have not considered dissipation or dispersion which are often met during propagation. Anisotropy has been a subject we have neglected. Also the layered structure which is questionable for the deep crust has not been considered here. Many extensions of the ray theory are possible and the future will show us how rich of consequences is this theory as it has already been in the past.

For applications, let us quote an obvious list. Locating earthquakes requires ray tracing between the expected position of the earthquake and stations at the Earth surface. The different slowness vectors at the source position allows to move the source towards a more accurate position which minimizes travel-time residues. At the same time, these initial slowness vectors gives the position onto the focal sphere of different stations: focal mechanisms can be deduced. Routine programs use mainly the layered approximation which is often a crude approximation for

many local networks. Synthesizing seismograms is also very important for the interpretation of seismic profiles along complex geological structures. Travel-time tomography with very sophisticated inversion schemes needs efficient ray tracing in order to give the most accurate image of the Earth interior. Going to diffraction tomography where the amplitude is also analyzed is a further step where ray theory brings its efficiency and its capacity of interpretation. These different subjects, which have been presented in other lectures, are those which should interest you for different applications of ray theory.

Acknowledgements

I would like to thank Andrea Morelli and Göran Ekstron for the opportunity to give a course on seismic ray tracing. Many discussions with Adam Dziewonski, Guust Nolet, Roel Snieder, Michael Weber, John Woodhouse help to clarify somehow this difficult subject as well as interventions of students attenting this course at Erice. A very helpful review has been performed by David Gubbins. This work has its root when I was in Paris working with Raùl Madariaga and Véronique Farra. I thank them for continuous discussions. I would like to thank A. Dziewonski and W.-J. Su for providing me the Figure 6.4.

Finally, without the support of the Institut Universitaire de France, this work would not have been performed.

REFERENCES

ABDULLAEV, S.S. (1993): *Chaos and dynamics for rays in waveguide media* (Gordon and Breach Science Publishers, Netherlands).

ALEKSEEV, A.S. and B.G. MIKHAILENKO (1980): The solution of dynamic problems of elastic wave propagation in inhomogeneous media by a combination of partial separation of variables and finite-difference methods, *J. Geophys.*, **48**, 161-172.

ALTERMAN, Z. and F. KARAL (1968): Propagation of elastic waves in layered media by finite difference methods, *Bull. Seism. Soc. Am.*, **58**, 367-398.

AKI, K. and P. RICHARDS (1980): *Quantitative Seismology: Theory and Methods* (W.H. Freeman, New York).

BADAL, J. and F.J. SERÓN (1986): *Elementos Finitos y Ondas Sismicas Superficiales* (Universidad de Zaragoza).

BEN-MENAHEM, A. and S.J. SINGH (1981): *Seismic Waves and Sources* (Springer-Verlag, New York).

BLEISTEIN, N. (1984): *Mathematical Methods for Wave Phenomena* (Academic Press, Inc., New York).

BOLT, B.A. (1982): *Inside the Earth* (W.H. Freeman and Co.).

BONNET, M. (1986): *Methodes des equations integrales regularisees en elastodynamique*, Thèse Ponts et Chaussées.

BORN, M. and E. WOLF (1986): *Principles of Optics* (Pergamon Press, New York).

BOUCHON, M. and K. AKI (1977): Discrete wave-number representation of seismic source wave fields, *Bull. Seism. Soc. Am.*, **67**, 259-277.

BOUCHON, M., M. CAMPILLO and S. GAFFET (1989): A boundary integral equation-discrete wavenumber representation method to study wave propagation in multilayered media having irregular interfaces, *Geophysics*, **54**, 1134-1140.

BREBBIA, C.A. (1978) *The Boundary Element Method for Engineers* (Pentech Press, London).
BREBBIA, C.A. (1984) *Topics in Boundary Element Research:* vol. 1 *Basic Principles and Application* – vol. 2 *Time-Dependent and Vibration Problems* (Springer-Verlag).
BULLEN, K.E. (1959): *An Introduction to the Theory of Seismology* (Cambridge University Press).
BURRIDGE, R. (1976): *Some Mathematical Topics in Seismology*, Courant Institut of Mathematical Sciences, New York University, New York.
CAMPILLO, M. (1987): Modeling of *SH*-wave propagation in an irregularly layered medium: application to seismic profiles near a dome, *Geophys. Prosp.*, **35**, 236-249.
ČERVENÝ, V. (1985): The application of ray tracing to the numerical modelling of seismic wave fields in complex structures, in *Handbook of Geophysical Exploration, Section 1, Seismic Exploration* (Geophysical Press, London), vol. 15A, 1-119.
ČERVENÝ, V. (1987): Ray tracing algorithms in three dimensional laterally varying layered structures, in *Tomography in Seismology and Exploration Seismics*, edited by G. NOLET and D. REIDEL (Hingham, Mass.).
ČERVENÝ, V. and R. RAVINDRA (1971): *Theory of Seismic Head Waves* (The University of Toronto Press, Toronto).
ČERVENÝ, V., J. LANGER and I. PŠENČIK (1974): Computation of geometrical spreading of seismic body waves in laterally inhomogeneous media with curved interfaces, *Geophys. J. R. Astron. Soc.*, **38**, 9-19.
ČERVENÝ, V., I.A. MOLOTKOV and I. PŠENČIK (1977): *Ray Method in Seismology* (Charles University Press, Praha).
ČERVENÝ, V., M.M. POPOV and I. PŠENČIK (1982): Computations of wave fields in inhomogeneous media – Gaussian beam approach, *Geophys. J. R. Astron. Soc.*, **70**, 109-128.
CHAPMAN, C.H. (1978): A new method for computing synthetic seismograms, *Geophys. J. R. Astron. Soc.*, **54**, 481-518.
CHAPMAN, C.H. (1985): Ray theory and its extensions: WKBJ and Maslov seismograms, *J. Geophys.*, **58**, 27-43.
CHAPMAN, C.H. and R. DRUMMOND (1982): Body-wave seismograms in inhomogeneous media using Maslov asymptotic theory, *Bull. Seism. Soc. Am.*, **72**, S277-S317.
CHAPMAN, C.H. and J.A. ORCUTT (1985): The computation of body wave synthetic seismograms in laterally homogeneous media, *Rev. Geophysics*, **23**, 105-163.
CHAPMAN, C.H. and R.T. COATES (1994): Generalized born scattering in anisotropic media, *Wave Motion*, **19**, 309-341.
DZIEWONSKI, A.M. (1996): Earth's mantle in three dimensions, in *Seismic Modelling of Earth Structure*, edited by E. BOSCHI, G. EKSTRÖM and A. MORELLI (Editrice Compositori, Bologna for Istituto Nazionale di Geofisica, Rome), 507-572 (this volume).
FARRA, V. and R. MADARIAGA (1987): Seismic waveform modeling in heterogeneous media by ray perturbation theory, *J. Geophys. Res.*, **92**, 2697-2712.
FARRA, V., J. VIRIEUX and R. MADARIAGA (1989): Ray perturbation theory for interfaces, *Geophys. J. Int.*, **99**, 377-390.
FARRA, V., R. MADARIAGA and J. VIRIEUX (1994): The ambiguity, in ray perturbation theory-comment, *J. Geophys. Res.*, **99**, 21963-21968.
FUCHS, K. and G. MÜLLER (1971): Computation of synthetic seismograms with the reflectivity method and comparison with observation, *Geophys. J. R. Astron. Soc.*, **23**, 417-433.
GAFFET, S. and M. BOUCHON (1989): Effects of two-dimensional topographies using discrete wavenumber-boundary integral equation method in *P-SV* cases, *J. Acoust. Soc. Am.*, **85**, 2277-2283.
GILMORE, R. (1981): *Catastrophe Theory for Scientists and Engineers* (John Wiley and Sons).
GOLDSTEIN, H. (1980): *Classical Mechanics* (Addison Wesley, Reading, Mass.).
HANYGA, A. (1989): *Ray Tracing in the Vicinity of a Caustic* (Bergen University).
HELMBERGER, D. (1996): Construction of synthetics for 2D structures; Core phases, in *Seismic Modelling of Earth Structure*, edited by E. BOSCHI, G. EKSTRÖM and A. MORELLI (Editrice Compositori, Bologna for Istituto Nazionale di Geofisica, Rome), 183-222 (this volume).
HIROSE, S. and J.D. ACHENBACH (1989): Time-domain boundary element analysis of elastic wave interaction with a crack, *Int. J. for Numer. Methods Eng.*, **28**, 629-644.

KEILIS-BOROK, V.I., A.L. LEVSHIN, T.B. YANOVSKAYA, A.V. LANDER, B.G. BUKCHIN, M.P. BARMIN, L.I. RATNIKOVA and E.N. ITS (1989): *Seismic Surface Waves in a Laterally Inhomogeneous Earth* (Kluwer Academic Publishers, Dordrecht).
KELLY, K.R., R.W. WARD, S. TREITEL and R.M. ALFORD (1976): Synthetic seismograms: a finite-difference approach, *Geophysics*, **41**, 2-27.
KLIMEŠ, L. and M. KVASNIČKA (1994): 3D networking ray tracing, *Geophys. J. Int.*, **116**, 726-738.
KOSLOFF, D. and E. BAYSAL (1982): Forward modeling by a Fourier method, *Geophysics*, **47**, 1402-1412.
KOSLOFF, D., M. RESHEF and D. LOEWENTHAL (1984): Elastic wave calculations by the Fourier method, *Bull. Seism. Soc. Am.*, **74**, 875-891.
KRAVTSOV, Y.A. and Y.L. ORLOV (1990): *Geometrical Optics of Inhomogeneous Media* (Springer-Verlag, New York).
LANDAU, L. and E. LIFCHITZ (1969): *Mécanique* (Mir edition, Moscou).
LUDWIG, D. (1966): Uniform asymptotic expansion at a caustic, *Comm. Pure Appl. Math.*, **29**, 215-250.
LUNEBERG, R.K. (1944): *Mathematical Theory of Optics* (Brown University, Providence, R.I.).
LYSMER, J. and L.A. DRAKE (1972): *A Finite Element Method for Seismology in Methods in Computational Physics* (Academic Press, Inc.).
MADARIAGA, R. (1984): Gaussian beam synthetic seismograms in a vertically varying medium, *Geophys. J.R. Astron. Soc.*, **79**, 589-612.
MIKAELIAN, A.L. (1980): Self-focusing media with variable index of refraction, in *Progress in Optics XVII* (Editor E. Wolf, North-Holland).
MOORE, B.J. (1994a): Analytical solutions for the ray perturbation in depth-varying media, *Geophys. J. Int.*, **114**, 281-288.
MOORE, B.J. (1994b): Simple analytical Green's for ray perturbations in layered media, *Geophys. J. Int.*, **115**, 1137-1142.
MORSE, P.M. and H. FESHBACK (1953): *Methods of Theoretical Physics* (Mc-Graw-Hill Book Company, Inc., New York).
MOSER, T.J. (1991): Shortest path calculation of seismic rays, *Geophysics*, **56**, 59-67.
MOSER, T.J., G. NOLET and R. SNIEDER (1992): Ray bending revisited, *Bull. Seism. Soc. Am.*, **82**, 259-288.
MOSER, T.J., T. VAN ECK AND G. NOLET (1992): Hypocenter determination in strongly heterogeneous earth models using the shortest path method, *J. Geophys. Res.*, **97**, 6563-6572.
PODVIN, P. and I. LECOMTE (1991): Finite differences computation of travel times in very constrated velocity models: a massive parallel approach and its associated tools, *Geophys. J. Int.*, **105**, 271-284.
POPOV, M. M. (1982): A new method of computation of wave fields using Gaussian beams, *Wave Motion*, **4**, 85-97.
RIZNICHENKO, Y.V. (1946): Geometrical seismics of layered media. Trudy Inst. Theor. Geophysics, vol. II, *Izd., An SSSR*, Moscow (in Russian).
SHERIFF, R.E. and L.P. GELDART (1983a): History, theory and data acquisition, in *Exploration Seismology* (Cambridge University Press).
SHERIFF, R.E. and L.P. GELDART (1983b): Data-processing and interpretation, in *Exploration Seismology* (Cambridge University Press).
SNIEDER, R. and M. SAMBRIDGE (1992): Ray perturbation theory for travel times and ray paths in 3D heterogeneous media, *Geophys. J. Int.*, **109**, 294-322.
SNIEDER, R. and M. SAMBRIDGE (1993): The ambiguity in ray perturbation theory, *J. Geophys. Res.*, **98**, 22021-22034.
STOFFA, P. (1989): *Tau-p: a plane wave approach to the analysis of seismic data* (Kluwer Academic Publishers, Dordrecht).
SU, W.-J., R.L. WOODWARD and A.M. DZIEWONSKI (1994): Degree 12 model of shear velocity heterogeneity in the mantle, *J. Geophys. Res.*, **99**, 6945-6980.
TELFORD, W.M., L.P. GELDART, R.E. SHERIFF and D.A. KEYS (1976): *Applied Geophysics* (Cambridge University Press, Cambridge).
THOMSON, C.J. (1989): Correction for grazing rays in 2D seismic modelling, *Geophys. J.*, **96**, 415-446.

THOMSON, C.J. and C.H. CHAPMAN (1985): An introduction to Maslov's asymptotic method, *Geophys. J.R. Astron. Soc.*, **61**, 729-746.
VIDALE, D. (1988): Finite-difference calculation of travel time, *Bull. Seism. Soc. Am.*, **78**, 2062-2076.
VIRIEUX, J. (1984): SH-wave propagation in heterogeneous media: velocity-stress finite-difference method, *Geophysics*, **49**, 1973-1957.
VIRIEUX, J. (1986): PSV-wave propagation in heterogeneous media: velocity-stress finite-difference method, *Geophysics*, **51**, 889-901.
VIRIEUX, J. and G. EKSTRÖM (1991): Ray tracing on a heterogeneous sphere by Lie series, *Geophys. J. Int.*, **104**, 11-27.
VIRIEUX, J. and V. FARRA (1991): Ray tracing in 3D complex isotropic media: an analysis of the problem, *Geophysics*, **16**, 2057-2069.
VIRIEUX J., V. FARRA and R. MADARIAGA (1988): Ray tracing in laterally heterogeneous media for earthquake location, *J. Geophys. Res.*, **93**, 6585-6599.
WAIT, J.R. (1981): *Wave Propagation. Theory* (Pergamon Press).
WANG, Z., F.A. DAHLEN and J. TROMP (1993): Surface wave caustics, *Geophys. J. Int.*, **114**, 311-324.
WEBER, M. (1988): Computation of body-wave seismograms in absorbing 2D media using the gaussian beam method: comparison with exact methods, *Geophys. J.*, **92**, 9-24.
WHITE, B.S., A. NORISS, A. BAYLISS and R. BURRIDGE (1987): Some remarks on the gaussian beam summation method, *Geophys. J.R. Astron. Soc.*, **89**, 579-636.
WITTLINGER, G., G. HERQUEL and T. NAKACHE (1993): Earthquake location in strongly heterogeneous media, *Geophys. J. Int.*, **115**, 759-777.
WUNSCH, C. (1987): Acoustic tomography by hamiltonian methods including adiabatic approximation, *Rev. Geophys.*, **25**, 41-53.
YEDLIN, M.J., B.R. SEYMOUR and B.C. ZELT (1990): Comparison of the WKBJ and truncated asymptotic methods for an acoustic medium, *Geophys. J. Int.*, **101**, 49-60.
YILMAZ, Ö. (1987): *Seismic Data Processing* (SEG Publications).

SEISMIC MODELLING OF EARTH STRUCTURE
Eds. Enzo Boschi, Göran Ekström and Andrea Morelli

7

Portable broadband seismology: results from an experiment in New Zealand

DAVID GUBBINS
Department of Earth Sciences, Leeds University, Leeds LS2 9JT, U.K.

7.1 Instrumentation, deployment, and database

7.1.1 *Modern field seismology*

Two separate technological advances made in the last 5 years have allowed us to collect observatory-quality seismic data from affordable, temporary arrays. One was the development of robust instruments with stable response characteristics over a wide range of frequencies, including surface wave frequencies. Their essential characteristic is ease of installation: an expensive site requiring, for example, mains power and precise temperature and pressure control would defeat the object of portability. The other was the advent of cheap mass storage to preserve the enormous volume of data these instruments produce, particularly when running continuously rather than in triggered mode. We now think nothing of using hard disks with a capacity of 1 Gbyte, backed up on cheap tapes holding several Gbytes each. A large dynamic range is needed to preserve the full range of seismic amplitudes, from emergent body wave arrivals to surface waves. Analogue systems could not record both *P* and surface waves on the same trace and the signal was therefore split into short period and long period recordings, with different gains and sampling frequencies. This restricted seismic studies either to permanent observatory sites, which are not always in ideal locations of interest or even sited with earthquake seismology in mind (indeed the first permanent arrays, such as NORSAR, were deliberately sited in uninteresting areas so as to reduce site effects on the signals), or to field arrays with short-period instrumentation, usually designed for specific local or regional studies, run in triggered mode. Triggering invariably leads to a loss of interesting data, and central recording is essential in preventing spurious triggers from events close to one of the stations. The new technology means that we can now put the "observatories" where we want them, pro-